



Working Paper 111-2021 | June 2021

Measuring and Pricing Cyclone-Related Physical Risk under Changing Climate

Confidence
must be earned

Amundi

ASSET MANAGEMENT

Measuring and Pricing Cyclone-Related Physical Risk under Changing Climate

Abstract

Théo Le Guenedal

Amundi Quantitative
Research
CREST-ENSAE, IP Paris
theo.leguedal@amundi.com

Philippe Drobinski

LMD-IPSL
Ecole polytechnique - IP
Paris, ENS - PSL Université,
Sorbonne Université, CNRS,
France
*philippe.drobinski@lmd.
polytechnique.fr*

Peter Tankov

CREST-ENSAE, IP Paris
peter.tankov@ensae.fr

We propose a statistical methodology to quantify the financial implications of tropical cyclone-related physical risks implied by climate change. To address the sensitivity of disaster intensity to climate change, we provide a Monte Carlo methodology to generate synthetic cyclones consistent with climate scenarios of the Couple Model Intercomparison Project (CMIP5). Sovereign exposure and vulnerability assessments in principal tropical cyclone basins are based on projections of population densities in shared socioeconomic pathways coupled with downscaled physical asset values constructed using mixed data along with locally calibrated damage functions. Finally, we compute the direct climate impact on emerging countries' bond spreads using the spread sensitivity to the debt to GDP ratio, assuming that damage costs are financed by issuing new government debt. We find that the 'business as usual' RCP8.5 concentration scenario coupled with the 'middle road' shared socioeconomic pathway (SSP2) leads to global average annual damages 142% larger than in the concentration scenario RCP2.6 allowing to remain under 2°C warming. In terms of emerging market impact, we estimate that in 2070-2100, the impact of extreme cyclones on the bond spread of most vulnerable countries will up to 200 bps higher in the RCP8.5 pathway than in the 2°C baseline. In every step of our assessment, we quantify the impact of model uncertainty on our results using 7 different climate models from the CMIP5 database.

Keywords: Climate change, physical risk, cyclone, sovereign risk, Monte Carlo simulation, damage modeling

JEL classification: Q54, C63, H63

Acknowledgement

The authors are very grateful to Mohamed Ben Slimane, Roberta Fortes, Esther Law, Florian Raymond, Thierry Roncalli, Takaya Sekine and Lauren Stagnol for helpful comments.

About the authors



Théo Le Guenedal

Théo Le Guenedal joined the Quantitative Research team of Amundi in December 2018 after his internship dedicated to the performance of ESG investing in the equity market. He is currently working on a broader research project on the “Integration of ESG Factors and Climate Risks in Asset Allocation Strategies”. At this occasion, Théo and his co-author Vincent Bouchet received the GRASFI Best Paper Prize for Research on Climate Finance (sponsored by Imperial College London), for their paper “Credit risk sensitivity to carbon price”. Prior to that, Théo graduated from Ecole Centrale Marseille with a specialization in Mathematics, Management, Economics and Finance. He also holds a master’s degree in mathematics and Applications from Aix-Marseille University. In 2017, Théo was awarded the postgraduate diploma “Engineers for Smart Cities” from the Mediterranean Institute of Risk, Environment and Sustainable Development and a master degree in Economic Management from the School of Economics and Business of Nice Sophia Antipolis University.



Philippe Drobinski

Philippe Drobinski is the director of the Laboratoire de Météorologie Dynamique de l’Institut Pierre Simon Laplace. He is research director at CNRS and professor at Ecole Polytechnique. His research focuses on regional climate variability and trends in the Euro-Mediterranean region with a particular interest in water and energy resources. He has coordinated many national and international programs, including the international program HyMeX on the Mediterranean water cycle, which he represented within the World Climate Research Program. Since 2019, he is the founding director of the interdisciplinary center Energy4Climate, aiming to address the systemic complexity of the energy transition. He is the author of over 160 book chapters and articles in international peer-reviewed journals and is the coordinating lead author of the energy chapter of the 1st MedECC Assessment Report on Change climate and environment in the Mediterranean region. At the Ecole Polytechnique, he teaches master’s level courses on climate change and renewable energies and is responsible for an executive training program on the environment and energy management.



Peter Tankov

Peter Tankov is Professor of Quantitative Finance at ENSAE, the French national school for statistics and economic administration, having previously worked at Paris-Diderot (Paris 7) University and Ecole Polytechnique. He is a mathematician, specialist in applied probability and stochastic processes. His current research interests include quantitative finance, energy finance, and green and sustainable finance. Peter is the author of over 50 research articles on these and other topics and of the widely read book “Financial Modelling with Jump Processes”. He is the recipient of the 2016 Best Young Researcher in Finance Award of the Europlace Institute of Finance and the principal investigator of several national grants. Peter is the Scientific Director of the Green and Sustainable Finance Research Program at Louis Bachelier Institute, member of the board of directors of GRASFI, the Global Research Alliance for Sustainable Finance and Investment, and member of editorial boards of the main quantitative finance journals (Mathematical Finance, Finance and Stochastics and SIAM Journal on Financial Mathematics).

1 Introduction

The direct effects of global warming on the planet are unequivocal – melting of glaciers, rising sea levels, unstable climate conditions, expanding deserts – phenomena that have been comprehensively detailed by the Scientific Committee of the Intergovernmental Panel on Climate Change (IPCC) in their reports (Pachauri *et al.*, 2014; Solomon *et al.*, 2007). However, these environmental issues are only the tip of the iceberg of the consequences of climate change, which also encompass the effects of climate change on societies and economies.

The financial implications of climate change fall in two main categories. First, transition risks and opportunities are the financial consequences of the transition toward a low carbon economy. A large body of literature describes the transmission channels of transition risk to the financial markets (Battiston *et al.*, 2017; Battiston & Monasterolo, 2019). On the other hand, the second type of climate-related risk categorized as ‘*physical risk*’ has been less addressed in the literature. Indeed, if the global effort is too late or insufficient (Jewell & Cherp, 2020), societies will be threatened by more intense disasters, and financial assets will suffer greater losses. These risks are particularly hard to apprehend as they will likely materialize in the long-term and are subject to deep uncertainty.

In this article, our aim is to quantify *physical risks at the country level, and assess their impact on financial markets*. We focus on tropical cyclones and model explicitly the four main dimensions of the problem: (i) the sensitivity of tropical cyclone intensity to climate change, (ii) the exposure level of the countries to the tropical cyclone risk, (iii) the vulnerability (amount of losses which may be caused by the tropical cyclone to the exposed assets) and (iv) pricing of the tropical cyclone risk by the financial markets.

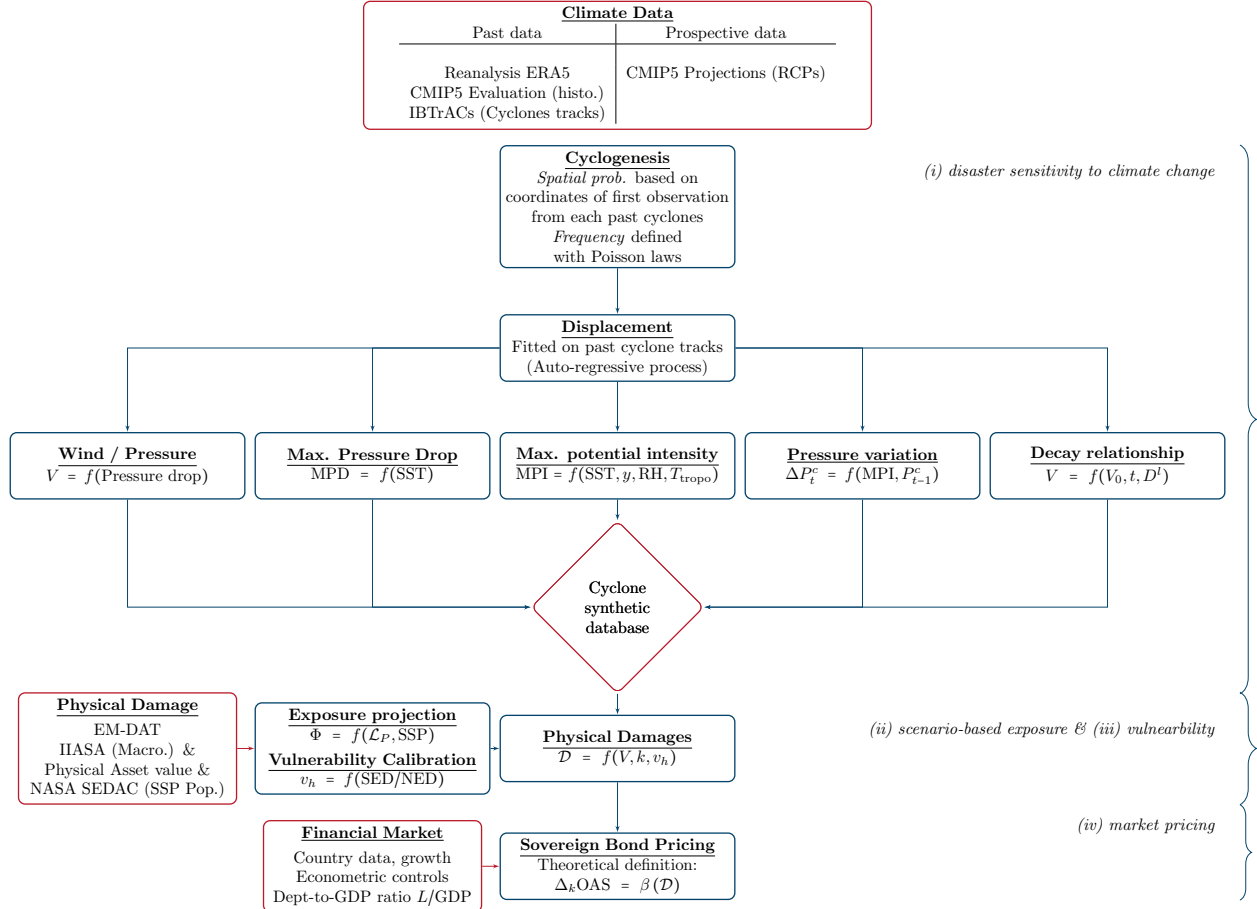
To address the first dimension, we provide a reproducible methodology to generate future cyclones from climate data inspired by Bloemendaal *et al.* (2020). We define an integrated cyclone generator that can be launched on any climate projection from the Phase 5 Coupled Model Intercomparison Project (CMIP5). Regarding the second dimension, to define countries’ exposure while encompassing the diversity of scenarios proposed in the IPCC assessment framework, we use multiple sources. We define the current local downscaled physical asset value exposed to tropical cyclone risk as in Eberenz, Stocker, *et al.* (2020). Then, to determine the future physical asset value exposure we apply two correction factors to the current local physical asset value: a global macroeconomic GDP/population ratio based on the trajectory defined in Riahi *et al.* (2017), and a local scenario-based population distribution based on the grid defined in Jones and O’Neill (2020). The vulnerability dimension is determined as in Eberenz, Lüthi, *et al.* (2020) who designed regional specific damage functions in the CLIMADA project. Finally, to address the market pricing issue, we channel the expected damages to emerging countries credit spreads by assuming that damage costs are financed by issuing new government debt and using an econometric model of Hilscher and Nosbusch (2010) to estimate the impact of debt to GDP ratio on bond spread. Combining open data sources and methodologies allows us to propose a complete integrated physical tropical cyclone damage assessment framework with a financial pricing module.

To quantify the model uncertainty of future climate projections, we use a multi-model ensemble consisting of 7 general circulation models developed by different climatological centers around the world. This approach allows us to quantify the main sources of uncer-

tainty in our estimates, namely the natural climate variability (by simulating many years of synthetic cyclones), the model uncertainty and the socio-economic uncertainty taken into account through the use of RCP pathways and SSP scenarios.

The methodology of this paper is illustrated in Figure 1. We first construct a synthetic cyclone tracks database translating the relationship between the scenario-based sea-surface temperature rise and the change in cyclones intensity. To this end we first define a model of cyclone genesis, which describes the number of cyclones appearing each year in each basin (North Atlantic, East, West and South Pacific, North and South Indian). Once initiated, the cyclones start moving, following the dynamics defined using simple auto-regressive formulas. The local variables determining the genesis and evolution of cyclones are based on four statistical equations and one thermodynamic relationship, calibrated on climate data and historical cyclone tracks.

Figure 1: Framework of cyclone physical risks assessment



In the second step of our methodology, we define the geographical distribution of sovereign exposure, in each scenario. We use the framework of the shared-socioeconomic pathways (SSP) (Riahi *et al.*, 2017). These narratives are used in the IPCC development scenarios and provide a reference framework for risk assessment. To this end, we use the current downscaled

physical asset value from Eberenz, Stocker, *et al.* (2020) and the vulnerability of each region from Eberenz, Lüthi, *et al.* (2020). We then determine the projected exposure using local expansion factor from NASA Socioeconomic Data and Applications Center (SEDAC, Jones and O’Neill (2020)) and / or global GDP per capita variation factor from Riahi *et al.* (2017). We apply a localized damage function to the exposure and aggregate the losses along cyclone tracks to estimate the loss for each synthetic cyclone.

Finally, we integrate the future cyclones damage cost in the pricing of emerging sovereign debt. To price the financial consequences of climate change related to tropical cyclones, we consider that the costs are paid by issuing new government debt and use the sensitivity of the option adjusted spread to the debt ratio. We use the JP Morgan EMBI Index constituents to fit our relationship.

In the end, we construct a full financial risk model, based on thermodynamic and statistical relationships, calibrated on open source climate and socio-economic data. We find that socioeconomic factors are influential but that climate change has a major impact on the future potential damage. Using the projections currently available for the time horizon 2070-2100, the representative concentration pathways RCP45 and RCP85 and *middle road* shared socioeconomic pathway (SSP2) lead respectively to global average annual damages 76% to 142% higher than in the RCP2.6, concentration scenario allowing to maintain the global warming below 2°C. In terms of emerging market impact, and by 2070, we estimate that the maximum annual cyclone-related spread variation for countries within the JP Morgan EMBI Index could increase in high concentration pathways up to 200 bps for most vulnerable countries with respect to a 2°C baseline.

The paper is structured as follows: after a comprehensive literature review in Section 2, Section 3 details the synthetic cyclone track generation algorithm; Section 4 presents the scenario-based approach for downscaled exposure and the regional damage functions and Section 5 presents the implications of physical risks on emerging countries’ bond spread. A detailed description of the data sources and of the model, as well as some additional information on the different sources of uncertainty affecting our results are presented in Supplementary Material.

2 Related Literature

Our choice to focus on cyclones is motivated by the importance of their impact on the economy and human life, reasons why they have received considerable attention from meteorologists and academics from several other disciplines. Additionally, it has been demonstrated that climate change increases the intensity of cyclones in a measurable way. For instance, using the total dissipation of power integrated over the lifetime of the cyclone, Emanuel (2005) showed an increase of the intensity index of tropical cyclones over the 30-year period since the mid-1970s. Recently, Kossin *et al.* (2020) also demonstrated the increasing trend of major tropical cyclone threshold exceedance probability. This trend is most clearly observable in the Atlantic basin (Elsner *et al.*, 2008), but incompleteness of the observations may explain the difference with the other basins. The current scientific consensus on the impact of climate change on tropical cyclones was summarized as follows:

“Future projections based on theory and high-resolution dynamical models consistently suggest that greenhouse warming will cause the globally averaged intensity of tropical cyclones to shift towards stronger storms, with intensity increases of 2 to 11% by 2100. Existing modeling studies also consistently project decreases in the globally averaged frequency of tropical cyclones, by 6 to 34%. Balanced against this, higher resolution modeling studies typically project substantial increases in the frequency of the most intense cyclones” (Knutson *et al.*, 2010, p. 1).

The impact of climate change on tropical cyclones intensity is thus undeniable. In other words, super storms are going to be the new norm. However, while the relationship between the radiative forcing and the evolution of extreme winds is explicitly established in medium and high-resolution models (Bacmeister *et al.*, 2018; Timmermann *et al.*, 2020; Zarzycki *et al.*, 2016), the freely accessible global climate projections from coupled model intercomparison projects (CMIP) do not include a module resolving cyclones and more generally extreme events. To fill this gap, we propose to adapt the model of Bloemendaal *et al.* (2020) to generate future cyclone tracks under specific representative concentration pathways (RCP).

The literature on cyclone modeling builds upon the seminal contributions by Emanuel (1988) followed by Holland (1997) and Emanuel (1999). Risk assessments have been developed from hurricane potential intensity maps to assess the damage in the US and worldwide (Emanuel, 2011; K. Emanuel *et al.*, 2008). To facilitate cyclone risk assessment, Bloemendaal *et al.* (2020) recently developed a modeling framework to simulate realistic synthetic tropical cyclone tracks: the Synthetic Tropical cyclones geneRation Model (STORM). This model relies mostly on statistical relationships (DeMaria & Kaplan, 1994; James & Mason, 2005; Kaplan & DeMaria, 1995) and is slightly different from the thermodynamic approach generally proposed for cyclones intensity index (K. Emanuel *et al.*, 2008). We found that Bloemendaal *et al.* (2020) specification lacks parameters describing the variation of the maximum potential intensity (MPI) – local energy potential allowing cyclones to grow stronger – therefore we propose to further detail the thermodynamic definition of this energy potential integrating relative humidity and upper troposphere temperatures. This important adjustment leads to a more precise modeling of the link between cyclone intensity and climatological variables which in turn enables us to quantify the impact of climate change on future cyclones by using climate variables from the CMIP5 climate projections.

On the economic side, the assessment of future cyclone damages requires to take into consideration multiple socioeconomic factors (Noy, 2016; Pielke Jr *et al.*, 2008; Weinkle *et al.*, 2018; Weinkle *et al.*, 2012; Ye *et al.*, 2020), but also their potential dynamics in the scenario of interest. For instance, in 2012, the annual damage from tropical cyclones was USD 26 billion according to the international disaster database (EM-DAT). The value of the damage went up to reach USD 73 billion in 2020. The cost will naturally increase in 2100, due to rise of both population and wealth concentration in areas subject to cyclones; in addition, Mendelsohn *et al.* (2012) showed that climate change will likely increase the impact by USD 53 billion per year in 2100 compared to the baseline. This quoted paper uses a single emissions scenario and does not employ the shared socioeconomic pathways and representative concentration pathways framework to assess the losses. To fill this gap, we propose to integrate the local scenario-based expansion maps developed by the Socio-Economic Data Application Center (SEDAC). Moreover, Mendelsohn *et al.* (2012) provide

highly aggregated results and therefore this paper has no direct financial application. For the methodology to be valuable in financial applications, we must introduce higher resolution asset exposure. To this end we employ the downscaled physical asset value database detailed in Eberenz, Stocker, *et al.* (2020).

Physical climate risks have not been as well addressed in the financial literature as transition risks. One reason for this lesser consideration could be that the present value of natural disasters occurring in the long-term is strongly reduced by a too high effective discount rate, which is in line with what Carney (2015) called the *Tragedy of the Horizons*. Although the issue of including climate change in market prices concerns a growing number of players, the measurement of damage costs is currently mainly addressed in the insurance market and the underlying methodologies cannot be readily applied to pricing financial assets. However, we show in this paper that these methodologies of direct damage measurement can be embedded as an intermediate step in financial scenario analysis.

Despite the lack of general methodology, practitioners have started to take some physical risks into consideration. In particular, local exposures to tropical cyclones are already priced, through the cat-bond market (Bantwal & Kunreuther, 2000; Morana & Sbrana, 2019) and/or relative spread of the states and local issuers in the municipal bonds markets. For example, Harvey and Irma clearly impacted the price of the cat-bond when they made landfall in the United States in 2017. Dimov and Parsons (2021) study the impact of historical cyclone landfall on the equity performance of manufacturers owning facilities located in the region affected by a given storm. For U.S. companies, they observed both “*a statistically significant negative pre-landfall drift and a significant positive post-landfall drift*”. On the academic side, Lanfear *et al.* (2019) also showed that stock markets responded to storm information using an event study approach. These studies suggest that tropical cyclones are good candidates for measuring the impact of climate change on portfolios.

At a sovereign level, the macroeconomic literature on sovereign default relies on dynamic general equilibrium models and on the seminal paper of Eaton and Gersovitz (1981). Recently, Mallucci (2020) proposed to assess the impact of disasters using this framework on Caribbean sovereign islands. The author finds that disaster risk reduces government’s ability to issue debt and that climate change further restricts government’s access to financial markets. The downside of the use of dynamic general equilibrium modeling framework is that it makes the assessments complex to transpose at a portfolio level. Indeed, to our knowledge, there is no integrated methodology describing the full transmission channel of the physical risk to asset prices and allowing to evaluate the physical risk at a portfolio level. To fill this gap, we propose to apply Hilscher and Nosbusch (2010) econometric specification to estimate how physical risk affects the option-adjusted-spreads (OAS) of emerging countries through the impact of direct damage on the debt-to-GDP ratio. Because of the higher vulnerability of emerging countries, we decide to focus on the constituents of the JP Morgan EMBI Index.

A number of recent articles and reports address the impact of climate change on sovereign default risk (Beirne *et al.*, 2020; Klusak *et al.*, 2021; Volz *et al.*, 2020). In particular, the report (Volz *et al.*, 2020) (see Table 4 therein) identifies multiple transmission channels through which physical and transition climate risks may impact sovereign bond spreads and default probabilities. Out of these channels, we focus on the fiscal impact of climate-related disasters, and more specifically tropical cyclones, and provide a methodology for assessing

the intensity of this impact under future warming and development scenarios. Beirne *et al.* (2020), show, through econometric analysis, that climate risk vulnerability and resilience are already significant determinants of the sovereign bond spreads. The article (Klusak *et al.*, 2021), which is perhaps closest in spirit to our study, simulates the effect of climate change on sovereign credit ratings under alternative warming scenarios. Their methodology is based on a statistical rating prediction model, combined with a macroeconomic growth model to project the impacts of global warming on GDP. By contrast, our aim is to analyse the impact of physical risks on sovereign bond spreads directly, by evaluating economic damage from synthetic future cyclones, without making reference to integrated assessment models. Indeed, the use of such models to evaluate future climate damages is still sometimes seen as controversial in the literature (Auffhammer, 2018; Pindyck, 2017).

3 Synthetic cyclone generation model

In this section, we detail the construction of random synthetic cyclone tracks consistent with different representative concentration pathways.

3.1 Climate and cyclone track data

Training a cyclone generator algorithm requires two types of data: the recorded tracks of past cyclones and the climate conditions in which these cyclones occurred. Combining the two allows to extrapolate the relationships between the climate conditions and the probability and intensity of the cyclones (Figure 2). These relationships, combined with the projections of future climate, then allow to generate realistic synthetic future cyclones. We employ the following databases:

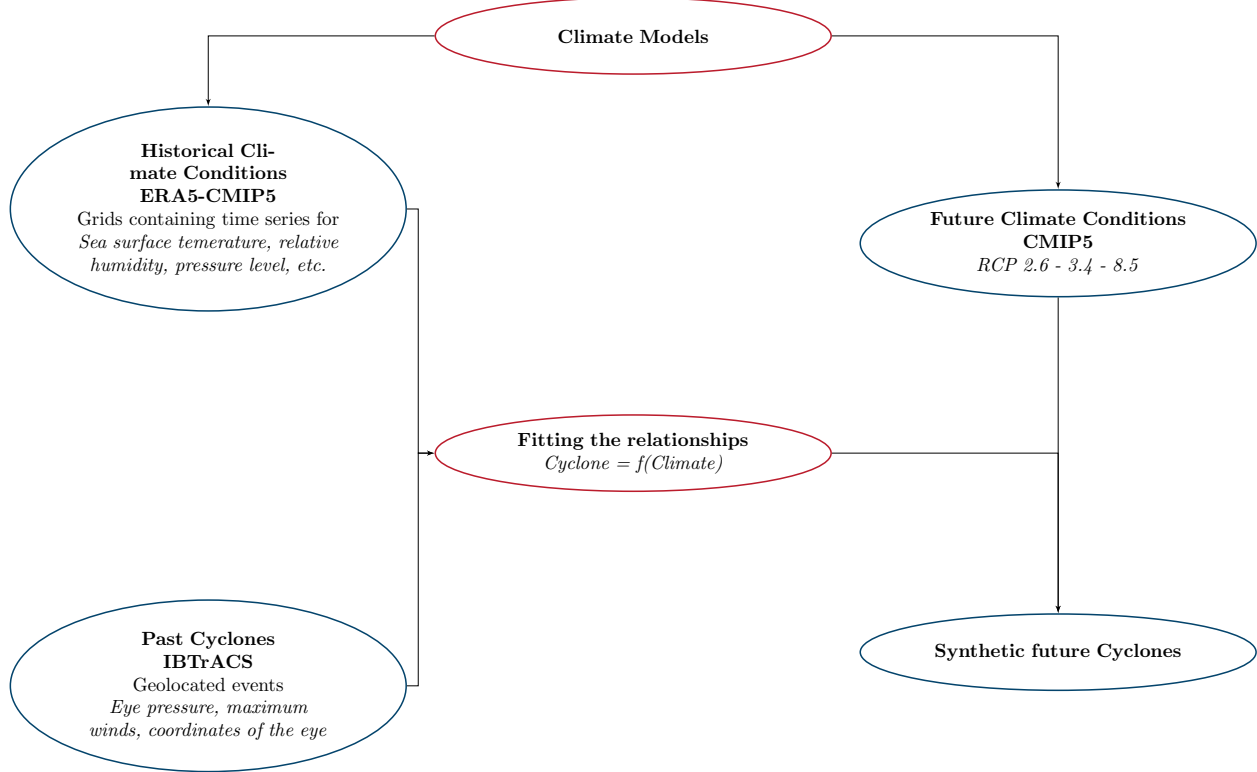
- For observed cyclone tracks we use the International Best Track Archive for Climate Stewardship (Knapp *et al.*, 2010) database (IBTrACS). This database presents the advantage to provide a standardized report of cyclones worldwide.

Cyclone tracks are reported on a 3 hour basis, with the measured central pressure, winds and radius to maximum winds. From this database we extract the wind speed, pressure and coordinate variations of cyclone tracks.

- The past climate data¹ is retrieved from ERA5 reanalysis database. We extract monthly mean sea level pressure (MSLP), monthly mean sea surface temperature (SST), relative humidity (RH), and tropopause temperature (T_{tropo}), i.e. temperature corresponding to atmospheric pressure around 50 hPa.
- To estimate the sensitivity of tropical cyclones intensity to climate change we use the future climate projections of the Coupled Model Inter-comparison project (Phase 5) models (Taylor *et al.*, 2012). We use the global climate projections in the climate data store (CDS), which is a quality-controlled subset of the wider CMIP5 dataset.

¹Climate data is available on the Copernicus Climate data store: <https://cds.climate.copernicus.eu/>.

Figure 2: Understanding cyclone generator data dependency



To take into account the potential biases in the climate models, we use models from multiple climate centers: NASA, Goddard Institute for Space Studies (GISS-E2-H, USA), Institut Pierre Simon Laplace (IPSL-CM5A-NR, France), Bureau of Meteorology - Commonwealth Scientific and Industrial Research Organisation (ACCESS1-0, BoM-CSIRO, Australia), Beijing Climate Center (bcc-csm1-1-m, China), Institute of Numerical Mathematics (inmcm4, Russia), Norwegian Climate Centre (NorESM1-ME, Norway), Canadian Centre for Climate Modelling and Analysis (CanESM2, Canada), according to the availability of the runs for the configurations of interest. Indeed, while the seven models are available for the historical period and Representative Concentration Pathway 8.5W/m² (RCP85), the CCCMA model is not available for RCP45, and only the IPSL, CCCMA, NCC and BCC models climate projections are available for RCP26. The different runs (r) of each models are derived from different initial conditions (i) and different physical parameters (p). These three parameters define the ensemble. The difference between ensembles is characteristic of the internal variability of the model. We use the ensemble ‘r1i1p1’ because it is available for the largest number of models in the configurations studied.

3.2 Cyclone generation model

Our model follows Bloemendaal *et al.* (2020) with some important adjustments. This paper defines three main modeling steps: genesis, displacement of the eye and calibration of the cyclone properties. The entire model relies on statistical relationships (DeMaria & Kaplan, 1994; James & Mason, 2005; Kaplan & DeMaria, 1995). This simulation method is slightly different from the purely thermodynamic approach advocated by Kerry Emmanuel models (Emmanuel, 1999; K. Emanuel *et al.*, 2008).

The main difference in our specification compared to Bloemendaal *et al.* (2020) is that we use a different local definition of maximum available thermodynamic intensity (MPI). In particular, we use relative humidity and tropopause temperature (50hPa), allowing for better calibration of cyclone properties. The main goal of this section is to present the process allowing to generate synthetic tracks properties i.e. maximum wind (V) and central pressure (P_c) at each step of coordinates latitude y , longitude x , and time t , given the climate conditions – sea surface temperature (SST), mean sea level pressure (MSLP), tropopause temperature (T_{tropo}), and relative humidity (RH) extracted from climate models.

Cyclone genesis Although in the literature there exist models relating the frequency of cyclones with the local atmospheric variables such as vertical shear, vertical instability and mid-level moisture variables (DeMaria *et al.*, 2001; Gray, 1975), there is still too much uncertainty about how climate change will affect the frequency of cyclones to justify the integration of multiple additional variables at this step. For this reason, we choose to rely on a simple model based on past frequencies. The number of synthetic cyclones each year is therefore determined by the Poisson distribution in each basin, with parameter λ defined as the average number of cyclones per year in the historical data. In other words, we make an assumption that the climate change does not affect the frequency of tropical cyclones. Similarly, the temporal and spatial position of synthetic future cyclones (starting month, latitude and longitude) is generated by resampling the historical distribution of these variables.

Cyclone trajectories A rich literature focuses on cyclone tracking algorithms, and advanced models have been developed and compared by several authors, see e.g., Neu *et al.* (2013). Here, following Bloemendaal *et al.* (2020), we choose to implement a simple autoregressive model for cyclone coordinates. Following James and Mason (2005), the time evolution of the latitude and longitude of the cyclone center is described by the following stochastic dynamics:

$$\Delta_t x_t = a_0 + a_1 \Delta_t x_{t-1} + \varepsilon_{x_t} \quad (1)$$

$$\Delta_t y_t = b_0 + b_1 \Delta_t y_{t-1} + \frac{b_2}{y_t} + \varepsilon_{y_t} \quad (2)$$

$$\varepsilon_{x_t} \sim \mathcal{N}(\mu_{x,B}, \sigma_{x,B})$$

$$\varepsilon_{y_t} \sim \mathcal{N}(\mu_{y,B}, \sigma_{y,B})$$

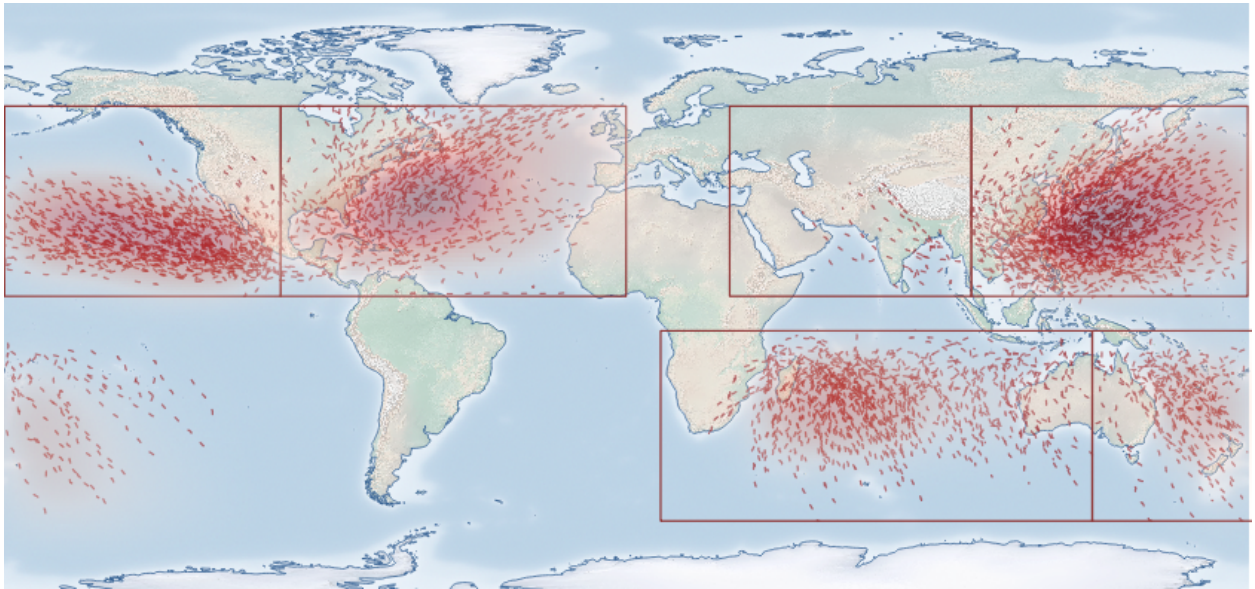
Here x_t and y_t are the latitude and longitude of the cyclone center sampled with a 3 hour time step; $\Delta_t x_t = x_t - x_{t-1}$, $\Delta_t y_t = y_t - y_{t-1}$, ε_{x_t} and ε_{y_t} are i.i.d. noises independent from one another and the constants a_0 , a_1 , b_0 , b_1 , b_2 , μ_x , μ_y , σ_x and σ_y are fitted on the IBTrACS

data independently for each basin by least squares regression. The non-linear term in the incremental variation of the latitude is justified as follows:

The empirical evidence is rather compelling for a tendency for cyclones to move away from the equator—a tendency that is fairly dominant at very low latitudes, but less strong elsewhere. This tendency can be simulated by adding to the cyclone latitude model a nonlinear term that provides a steeply increasing tendency for $\Delta y(t)$ to be directed southward as the cyclone approaches the equator. [...] The form chosen here varies inversely with latitude (James & Mason, 2005, p. 183).

This simple auto-regressive model provides acceptable results ($R^2 > 0.8$ and see Figure 3). We found this formulation sufficient for global financial assessment despite its lack of consideration for dependencies in the latitudinal and longitudinal variations (James & Mason, 2006).

Figure 3: Synthetic databases generated with ERA-5



Note: Samples of storms modeled based on ERA-5 reanalysis between 1970-2000.

Cyclone intensity The intensity of cyclones in our model is defined through the following five steps:

1. We describe the cyclone intensity through its central pressure P_t^c . Let V_t be the maximum 10-min sustained wind speed of the cyclone at time t (this variable is reported in IBTrACS dataset for historically observed cyclones). The wind-pressure relationship (WPR) is defined in Bloemendaal *et al.* (2020) for the whole cyclone database as follows:

$$V_t = a \cdot (\text{MSLP}(x_t, y_t, t) - P_t^c)^b \quad (3)$$

where $\text{MSLP}(x, y, t)$ is the mean sea level pressure at this time and location. This statistical approach mimics a first order estimation of gradient flow / hydrostatic equilibrium².

2. In the second step, we compute the local maximum potential intensity (MPI) following Holland (1997) and using thermodynamic relationships. This step differs from the specification of Bloemendaal *et al.* (2020). Our approach takes into account the additional energy potential due to the widening of temperature difference between sea surface and upper troposphere³. Following the theory of Emanuel (1988) and additional simplifications proposed in subsequent papers (Emanuel, 1991) summarized in Holland (1997), the thermodynamic version of the MPI definition in our model becomes:

$$\begin{aligned}
 \text{MPI}_t &= \text{MSLP}(x_t, y_t, t) \cdot e^{-X_t} & (4) \\
 X_t &= \frac{\mathcal{E}_t \cdot \text{SST}(x_t, y_t, t) \cdot \Delta S_t^m - \frac{f(y_t)^2 r_{env}^2}{4}}{R_d \cdot \text{SST}(x_t, y_t, t)} \\
 \mathcal{E}_t &= \frac{\text{SST}(x_t, y_t, t) - T_{\text{tropo}}(x_t, y_t, t)}{\text{SST}(x_t, y_t, t)} \\
 \Delta S_t^m &= R_d \ln \left(\frac{\text{MSLP}(x_t, y_t, t)}{P_{t-1}^c} \right) + \frac{L_v (q_{ct}^* - q_t^{env})}{\text{SST}(x_t, y_t, t)} \\
 q_{ct}^* &= \frac{3.08 \cdot \text{RH}_c}{P_{t-1}^c} \exp \left(\frac{17.67 (\text{SST}(x_t, y_t, t) - 273.15)}{\text{SST}(x_t, y_t, t) - 29.65} \right) \\
 q_t^{env} &= \frac{3.08 \cdot \text{RH}(x_t, y_t, t)}{\text{MSLP}(x_t, y_t, t)} \exp \left(\frac{17.67 (\text{SST}(x_t, y_t, t) - 273.15)}{\text{SST}(x_t, y_t, t) - 29.65} \right)
 \end{aligned}$$

where $\text{SST}(x_t, y_t, t)$ and $T_{\text{tropo}}(x_t, y_t, t)$ are respectively the sea-surface and tropopause (i.e. at 50 hPa or at an altitude of 20 km) temperatures, $\text{MSLP}(x_t, y_t, t)$ is the mean local sea level pressure, $\text{RH}(x_t, y_t, t)$ is the relative humidity, $f = 2\omega \sin(y_t)$ is a Coriolis parameter depending on the latitude, r_{env} is the distance between the eye and the area under regular conditions (fixed at 500km), q_{env} and q_c respectively are the specific humidity at environmental conditions and in the eye. ΔS^m is the difference of moist entropy between the environment and the storm center. We suppose $\text{RH}_c = 1$. All the variables and constants are given with their respective units in the Appendix A on page 43.

3. To prevent the depression from diverging, we cap it by the maximum pressure drop,

²See Chavas *et al.* (2017) and Knaff and Zehr (2007) for further details.

³Indeed, greenhouse gas emissions not only warm up the oceans, but also cool down the lower stratosphere. Quoting from (Butchart *et al.*, 2000): “*In the southern winter stratosphere the flux of wave activity from the troposphere increased, but any additional dynamical heating was more than offset by the extra radiative cooling from the growing total GHG concentration*”. The effects of anthropogenic emissions in general including ozone (Forster *et al.*, 2007) therefore converge toward a cooling effect of low stratosphere / upper troposphere (Ramaswamy *et al.*, 2006).

as function of the sea surface temperature:

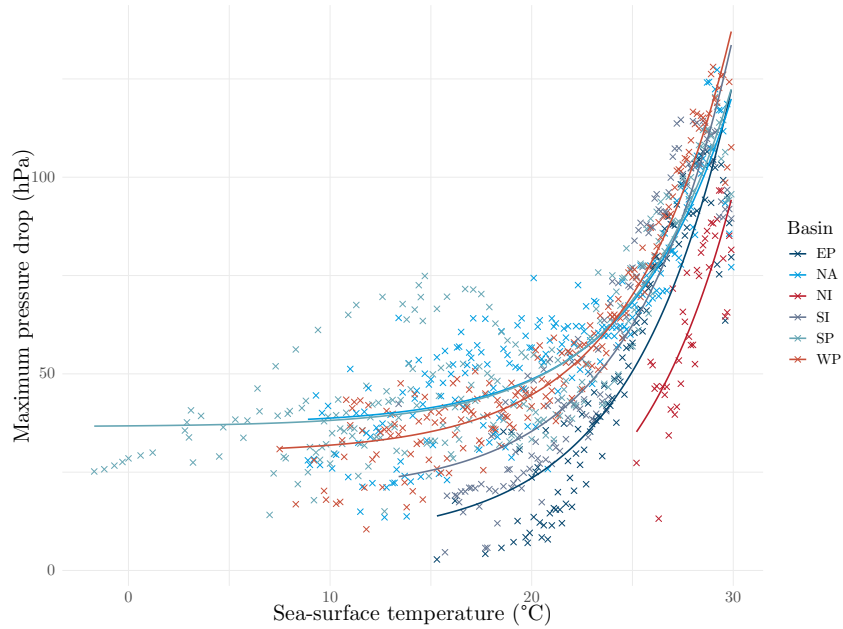
$$P_t^c := \max(P_t^c, \text{MSLP}(x_t, y_t, t) - \text{MPD}(\text{SST}(x_t, y_t, t))),$$

where the maximum pressure drop function is given by the following equation:

$$\text{MPD}(\text{SST}_b) = A + B \cdot e^{C(\text{SST}_b(x_t, y_t, t) - T_0)}, \quad T_0 = 30.0^\circ\text{C}, \quad (5)$$

which is fitted for each basin using the historical tracks and ERA5. This relationship is illustrated in Figure 4.

Figure 4: Sea-surface temperature max pressure drop relationship



4. The evolution of the central pressure depending on local MPI is described by the following autoregressive stochastic dynamics (James & Mason, 2005):

$$\begin{aligned} \Delta_t P_t^c &= c_0 + c_1 \Delta_t P_{t-1}^c + c_2 e^{-c_3 [P_t^c - \text{MPI}_t]} + \varepsilon_{P_t^c, t} \\ \varepsilon_{P_t^c, t} &\sim \mathcal{N}(\mu_{P^c}, \sigma_{P^c}) \end{aligned} \quad (6)$$

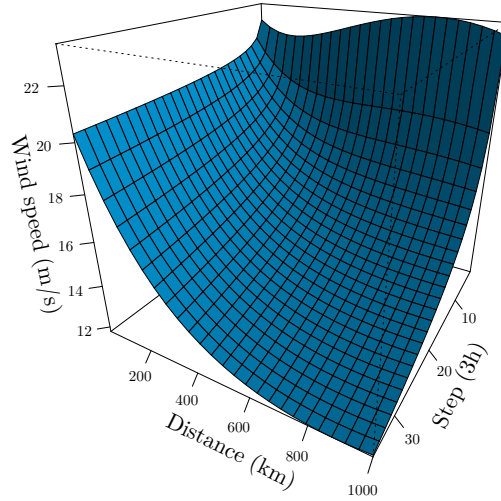
where the distance to maximum potential, $P_t^c - \text{MPI}_t$, enters as a non-linear term in the dynamic definition of the central pressure “*providing an increasing tendency for Δp to be positive as the central pressure approaches the mean MPI for the cyclone’s location*” (James & Mason, 2005, p. 183). The parameters are fitted on historical data using nonlinear least squares. This relationship channels the effect of global warming, affecting the maximum potential intensity, on the cyclone intensity. In other words, the incremental variation of the central depression of the cyclone is linked to the difference between the central pressure at time t and the potential available in the environment.

5. In the last step, we model the evolution of the cyclone after landfall. We fitted the decay function for each basin considering that “*Tropical cyclone intensity decreases as a function of the time and distance the tropical cyclone has covered whilst being over land*” (Kaplan & DeMaria, 1995):

$$\begin{aligned} V_{t_L} &= V_b + (R \cdot V_0 - V_b)e^{-\alpha t} - m(t_L) \left(\ln \frac{D^l}{D_0} \right) + b(t_L) \\ &= V(t_L, D^l, V_0) \end{aligned} \quad (7)$$

where D^l is the distance to coast, V_0 is the wind at landfall and t_L the time spent on land by the eye.

Figure 5: Decay of a cyclone making landfall with wind speed of 30 m/s (or 108km/h). This surface is obtained with the parameter fitted on IBTrACS data. This relationship is used after 3 time steps.



The function represented Figure 5 was fitted on IBTrACS using non-linear least squares. In our procedure, we use the global parameters: $R = 0.79$, $V_b = 15$ m/s, $\alpha = 0.044h^{-1}$, and $m(t_L) = \tilde{c}_1 t_L (t_{0,L} - t_L)$, $\tilde{c}_1 = 3.35 \cdot 10^{-4} m s^{-1} h^{-2}$, $t_L = 172h$, $b = d_1 t_L (t_{0,L} - t_L)$, $d_1 = -0.00186 m s^{-1} h^{-2}$ and $D_0 = 1$. The example provided on Figure 5 shows how a cyclone with a wind speed at landfall of 30 m/s rapidly decays over land.

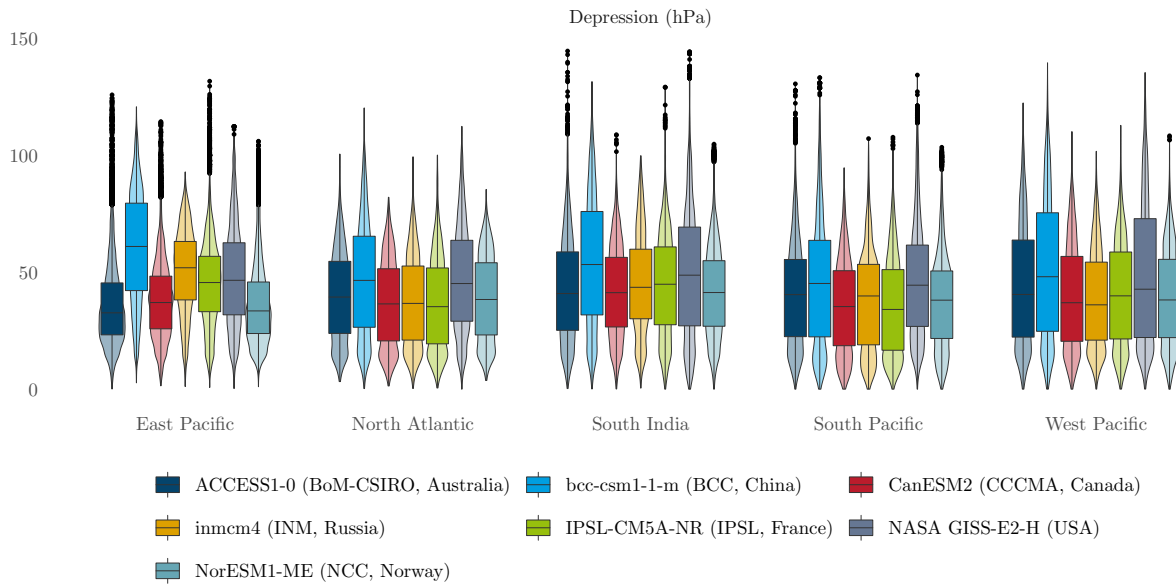
The full cyclone track generator Algorithm 1 is presented on page 45. The cyclone wind speed is initiated at 20 m/s and the initial pressure is determined from the WPR Equation (3). While the cyclone is over sea, the pressure evolution $\Delta_t P_c$ is determined from the dynamic Equation (6) based on the local MPI. To prevent the model from producing unrealistically low central pressure, we cap the maximum pressure drop using Equation (5).

While the cyclone is over sea, the wind is defined with the Equation (3). When the cyclone arrives on land the MPI is computed from the last known climate variables for three steps and the pressure keeps following the same relationship (6). After three steps (9h) on land, we start applying the decay relationship – Equation (7) – to define the wind. The variations of longitude and latitude are always defined using Equation (1) and Equation (2). We force cyclones to remain in their genesis basins in this exercise.

3.3 Generation of synthetic cyclones in representative concentration pathways

The properties of the cyclones are similar when this algorithm is used with CMIP5 climate data over the historical period (1980-2000). We use the following climate models: NASA GISS-E2-H (USA), IPSL-CM5A-NR (IPSL, France), ACCESS1-0 (BoM-CSIRO, Australia), bcc-csm1-1-m (BCC, China), inmcm4 (INM, Russia), NorESM1-ME (NCC, Norway), CanESM2 (CCCMA, Canada). The depression profiles simulated over the historical period are similar among the models (see Figure 6). The distribution of CMIP5 output is defined as the aggregation of outputs of all models.

Figure 6: Synthetic depression distribution in (CMIP5) models per basin over the historical period (1980-2000)

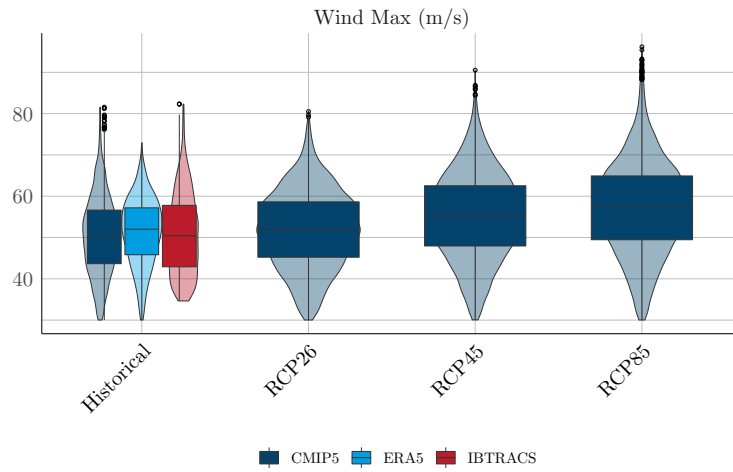


To measure to sensitivity of tropical cyclones to climate change we introduce the representative concentration pathways (RCPs) corresponding to the radiative forcing $2.6W/m^2$, $4.5W/m^2$ and $8.5W/m^2$ between 2070 and 2100. The synthetic cyclones were generated using RCP scenarios for the period between 2070 and 2100, where today’s action starts making a significant difference.

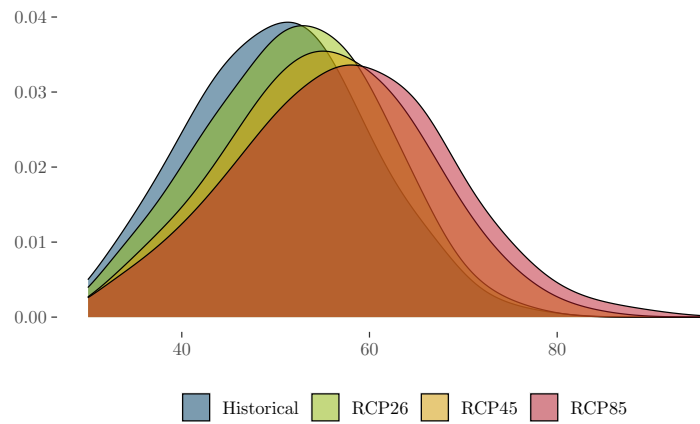
To focus on the main variable of interest Figure 7 compares the distributions of maximum winds from the synthetic tracks obtained with the same climate models over the periods 1980-2010 and 2070-2100 (with RCP85 pathway). An increase in cyclone intensity is clearly visible. For instance the average increase in the RCP45 and RCP85 compared to the historical data is respectively 9.5% and 13.5%, which is in line with the literature (Knutson *et al.*, 2010).

Figure 7: Tropical cyclone maximum wind sensitivity to climate change

(a) Comparing cyclones observed, generated with reanalysis and climate models maximum wind (m/s)



(b) Maximum wind density (CMIP5)



(c) Statistics of simulated wind

	Mean	St. dev	Median	1st Qu.	3rd Qu.	Max.
Historical	50,4	9,3	50,4	43,7	56,6	81,6
RCP26	52,0	9,4	52,1	45,2	58,6	80,5
RCP45	55,2	10,5	55,2	48,0	62,5	90,5
RCP85	57,2	11,3	57,4	49,5	64,9	96,2

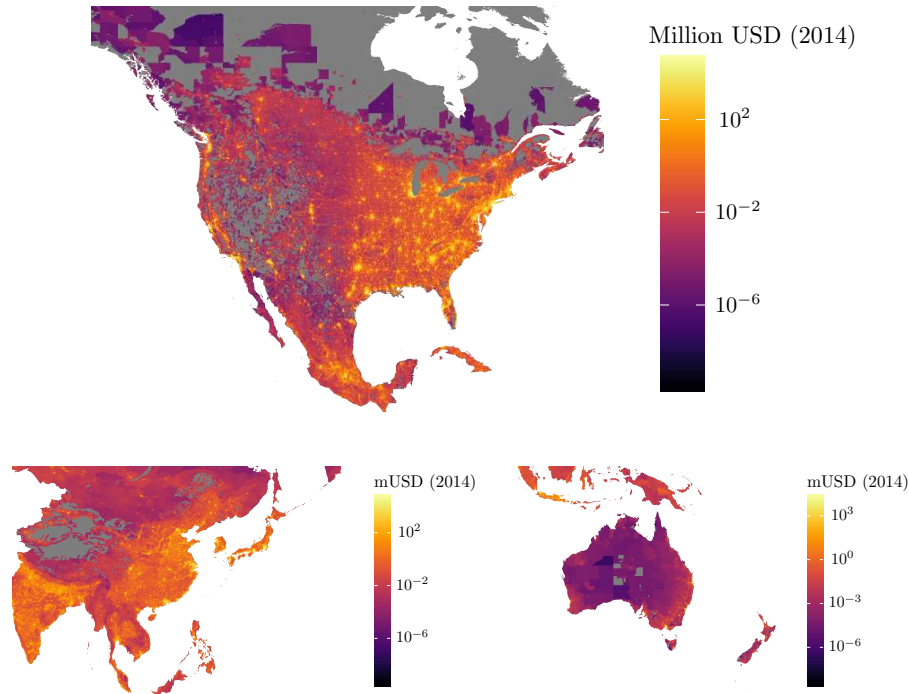
4 Sovereign exposure and vulnerability

In Section 3 we produced synthetic tracks translating both *probability* and *intensity* of the future tropical cyclones. In this section, we model asset *exposures* in multiple narratives and we introduce *vulnerability curves* to estimate the fraction of the value lost. This section is inspired by the literature associated to the CLIMADA project,⁴, which we combine with the future GDP and population projections.

4.1 Sovereign asset exposure

Current asset exposure To define the present-day physical asset exposure, we use the distribution of physical asset values on a high-resolution (30 arc-second) grid, estimated using a combination of nightlight intensity, population data, and global country indicators (Eberenz *et al.*, 2019, 2020). To illustrate this database, we display the local exposure in the major basins on Figure 8. We define the variable \mathcal{L}_P as the physical asset value exposed – defined with a 30 arc-second resolution – and re-aggregated on a one-eighth degree grid.

Figure 8: Physical asset values (in USD million per 1/32 degree)



Source: Eberenz, Stocker, *et al.* (2020)

Maps used in the assessment are obtained by summing the 30 arc-second ($\sim 1/120^\circ$) on tiles proportional to cyclone radius. In this Figure, we aggregated asset value on $1/32^\circ$ grid.

⁴Source code and data are available on GitHub at: <https://github.com/CLIMADA-project/CLIMADA-python/releases/tag/v1.5.1>.

Macroeconomic narratives The future exposure is sensitive to the scenarios of population growth and economic development. To take this into account, we use the framework of the shared-socioeconomic pathways (SSP) (Riahi *et al.*, 2017). These narratives are used in the IPCC development scenarios and provide a reference framework for risk assessment. Figure 9 displays the scenario-based projections of GDP and population in the five SSP, at the world level by the IIASA model⁵. We recall that the *middle road* pathway (SSP2) is used as the reference in most scenario analyses. It is an optimistic but plausible baseline in terms of economic and social resiliency, in which urbanization level is high and GDP and population are constantly increasing. On the other hand, the *rocky road* pathway (SSP3) presents totally different properties: decreasing GDP with strong increase of the population.

Scenario-based exposure metric To estimate future exposures along the cyclone track in each scenario, we use the downscaled estimation for the exposed wealth and the coefficients representing the change between the current state and the future scenario. The local physical exposure at the coordinates (x, y) at time t in a region j in scenario k is defined as follows:

$$\Phi(x, y, j, k, t) = \underbrace{F_{\text{GDP}}^{\text{cap}}(j, k, t)}_{\text{Global macro factor}} \cdot \underbrace{F_{\text{pop}}(x, y, k, t)}_{\text{Local factor}} \cdot \mathcal{L}_P(x, y). \quad (8)$$

This scenario-based exposure indicator is defined on a 30 arc-second grid.

The factor F_{GDP} is the projected GDP per capita growth for each region:

$$F_{\text{GDP}}^{\text{cap}}(j, k, t) = \frac{\text{GDP}(j, k, t)/\text{GDP}(j, t = 2020)}{P(j, k, t)/P(j, t = 2020)} \quad (9)$$

where P is the total population of the region. We use the most granular projections of GDP per capita variation curves (Figure 19 on page 46).

The factor F_{pop} is defined as follows:

$$F_{\text{pop}}(x, y, k, t) = \frac{p(x, y, k, t)}{p(x, y, t = 2020)} \quad (10)$$

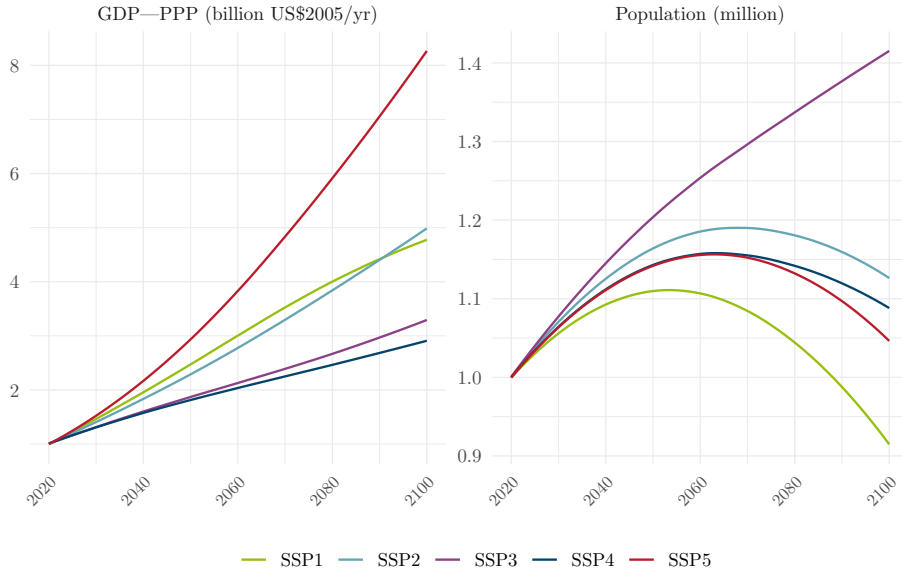
where $p(x, y, k, t)$ represents the local projections of population, available from the SEDAC database (Jones & O’Neill, 2020) with a one-eighth degree resolution. Figure 10 represents this multiplicative factor in the SSP2 (10a), SSP3 (10b), SSP4 (10c) and SSP5 (10d) in 2100.

4.2 Physical vulnerability

Explicit functions The relationship between the wind speed and the fraction of losses has been determined empirically from historical data using explicit damage functions of several forms. Prahl *et al.* (2019) compare these functions and describe their mathematical specification, extending their use to other natural hazards (Prahl *et al.*, 2016). Generic exponential functions for economic damage were used in Weitzman (2010) while Nordhaus (1993) used power law functions. However, the calibration of the function parameters on

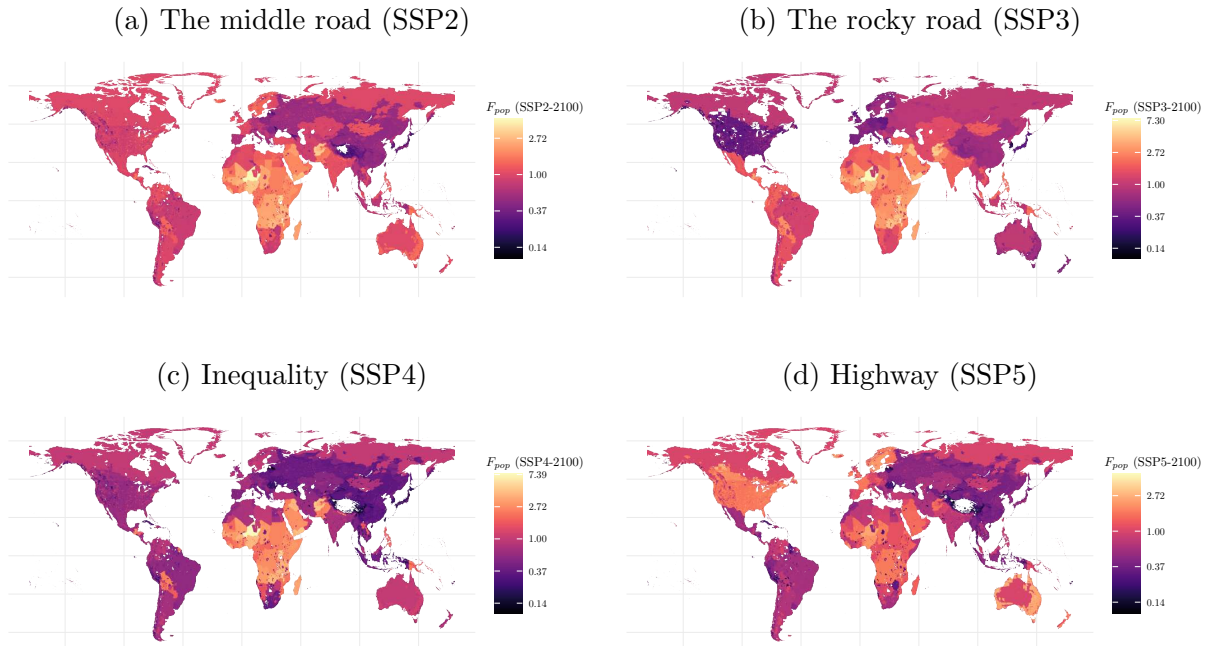
⁵Variables relative to SSPs are available here: <https://tntcat.iiasa.ac.at/SspDb/>.

Figure 9: World GDP and global population variation



Source: Riahi *et al.* (2017). This figure gives the global trends for GDP and population variation from 2020 to 2100. The regional projections of $\Delta_{t,k}y_{cap}(y, k, t)$ (see Equation (9)) are given on Figure 19 in the Appendix on page 46.

Figure 10: Variation of population exposure in 2100



The scenario-based population grid generation is detailed by Jones and O'Neill (2020) with a last version downscaled at 1km following Gao (2020). This population grid is available every 10 years. We use the closest value in the definition of the exposure.

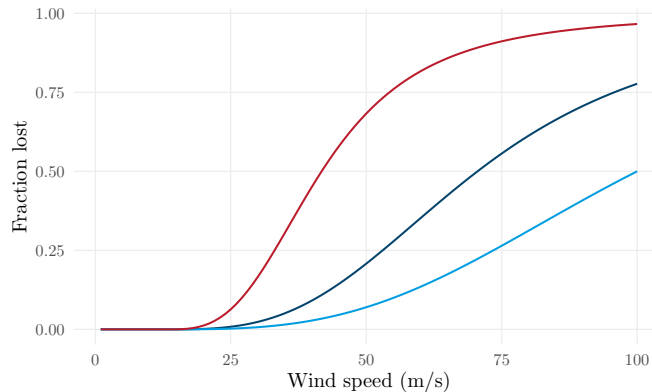
relevant data and the definition of their domain of validity is more important than their specific form.

Cyclone damages are generally assessed using a cubic functional of the wind speed, which corresponds to the intensity of the storm. For example, Pinto *et al.* (2012) studied the future loss potential in Europe using this type of formulation. To estimate the fraction of loss from a storm with sustained wind speed V , Emanuel (2011, p. 264) introduced the following formula:

$$f(V, v_h^j) = \frac{(\max(V - v_0, 0))^3}{(v_h^j - v_0)^3 + (\max(V - v_0, 0))^3} \quad (11)$$

where f is the fraction of the property value lost, $v_0 = 25.7$ m/s and v_h^j a parameter that needs to be calibrated for each region j .

Figure 11: Fraction of property value lost as a function of winds speed



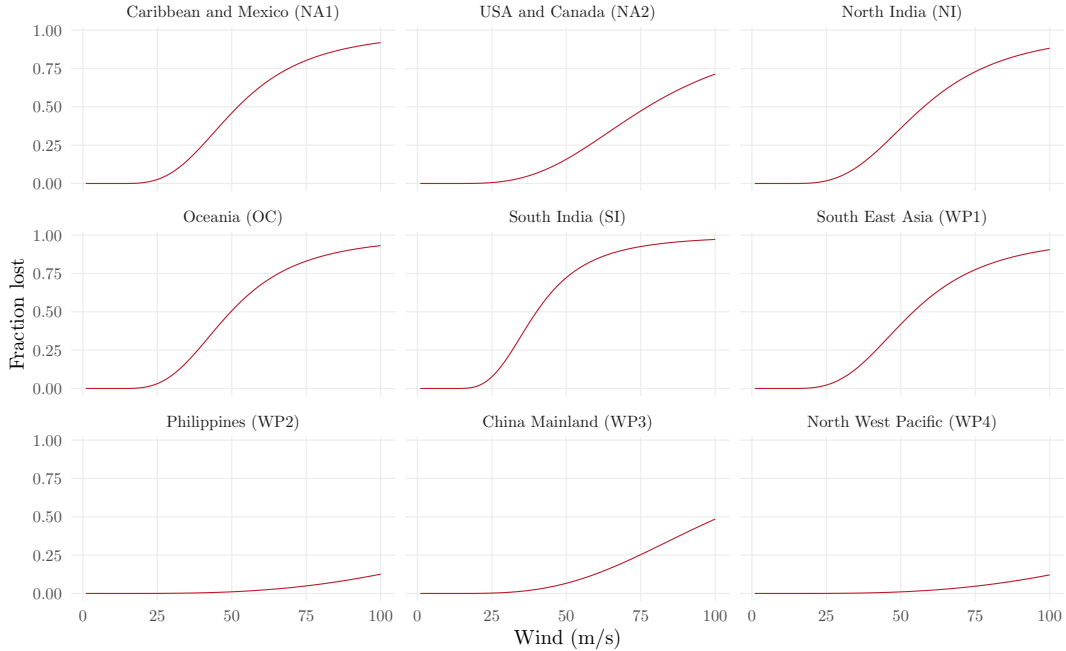
Source: Emanuel (2011, p. 264)

Using Equation (11) with $v_h^j = 50$ (red), 74.4 (dark blue) and 100 m/s (light blue).

Regional damage functions Using the reported damage estimates by the International Disaster Database (EM-DAT) (Guha-Sapir *et al.*, 2018) crossed with cyclone tracks (IB-TrACS), and geographic and socio-economic information along these tracks, Lüthi (2019) refined this approach using machine learning techniques. The aim to better describe local vulnerability and adaptation capacities. The CLIMADA module implements this approach (Aznar Siguan & Bresch, 2019; Bresch, 2017), filling the gap between bottom-up and top-down assessment. Based on this module, Eberenz, Lüthi, *et al.* (2020) introduced region-specific damage functions, that is used in the rest of this paper (see Figure 12). The functions were also calibrated on the downscaled physical asset exposure database (Eberenz, Stocker, *et al.*, 2020) previously introduced, which ensures the consistency of the assessment.

Damage along tracks The simulated damage for a given cyclone – in both IBTrACS and our synthetic tracks – is computed using the following three-step algorithm.

Figure 12: Regional Damage Functions



Source: Eberenz, Lüthi, *et al.* (2020). WP4: North West Pacific corresponds to Japan, South Korea, Macao, Hong-Kong, and Taiwan.

- First, a uniform grid with step given by the average cyclone radius is defined on the map of affected area. The cyclone track is linearly interpolated, and the tiles affected by the cyclone (containing a part of the interpolated path) are identified.
- Second, for each tile identified in the previous step, we retrieve the maximum wind speed V , and compute the proportion of wealth lost $f(V, v_h^j)$ using the relation (11) with the parameter given in Eberenz, Lüthi, *et al.* (2020).
- In the last step we compute the total simulated damage by aggregating the scenario-based downscaled exposure multiplied by the proportion of wealth lost on each tile over all tiles affected by the cyclone.

As a result of this algorithm, we obtain the total simulated damage $SED_i(j, k, t)$ caused by the i -th cyclone in region j for scenario k , simulated with climate variables for year t .

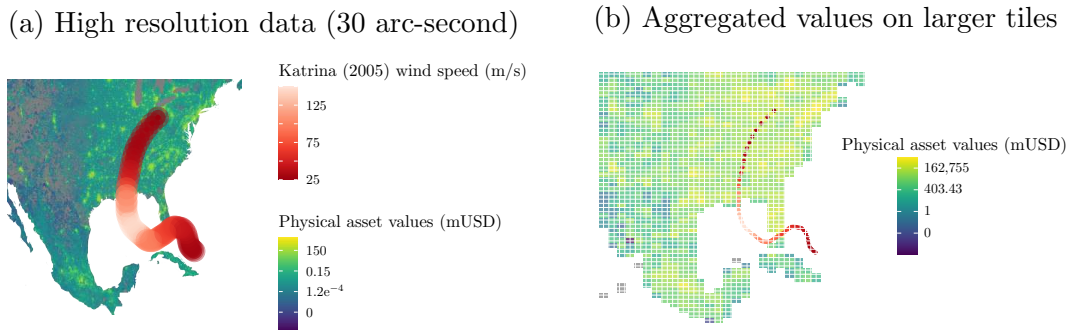
Finally, the cyclone damage cost in region j for scenario k and year t is simulated as follows:

$$\mathcal{D}(j, t, k) = \sum_i SED_i(j, k, t), \quad (12)$$

where the sum is taken over all cyclones occurring in a given year. This procedure can then be repeated many times to obtain the distribution of annual cyclone damages and compute other statistics such as the mean and quantiles of this distribution. Figure 13 provides an illustration of this process with Katrina (2005). Figure 13a represents the path of this storm

on high resolution physical asset value mapping. Figure 13b presents the aggregated values of physical exposure on larger resolution grid. This allows us to simplify the process in place in the CLIMADA module which is adapted in the context of a global sovereign exposure assessment.

Figure 13: Damage along track: example of Katrina (2005)

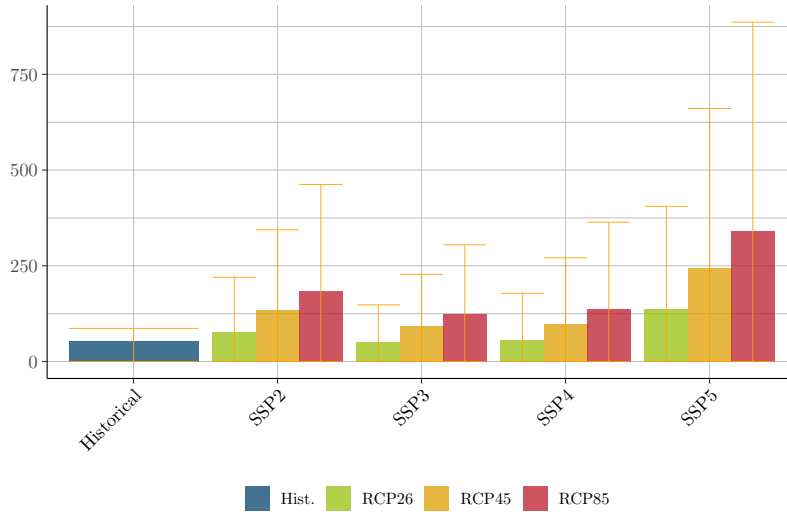


Results First, the historical annualized average damages were simulated with the current physical asset values and past climate data (see Figure 14). Over this period, the average annual damage was USD 53 billion, to compare with the 2020 annual cyclone damage cost of USD 73 billion worldwide. The maximum simulated annualized damage of USD 175 billion is consistent with the observed records. For instance, the total damages for the year 2005, after the tropical cyclone Katrina, were estimated at USD 181.6 billion. Our damage modeling specification thus provides estimations of the right order of magnitude for global annualized damage.

Future damage projections are sensitive to the scenario-based economic growth and population distribution. Figure 14 highlights that economic growth plays a key role in the expression of damage. By construction of the exposure indicator $\Phi(x, y, j, k, t)$, the scenarios in which the local impacted wealth increases the most are the scenarios with highest annualized damage. On the other hand, these results must be interpreted with caution. For example, one could question the consistency of the average annualized damage in the SSP5. Indeed, the two main dimensions used for shared socioeconomic pathways are *adaptation* and *mitigation*. The SSP5 corresponds to little mitigation, i.e. high mitigation challenge, but also high adaptation, i.e. low adaptation challenge. Therefore, annualized damage estimates in the SSP5 without considering adaptation may not be particularly relevant in this case. Our assessment can however be used to calibrate adaptation measures, in a context where the mitigation challenges are higher than those of adaptation.

By 2070, in the RCP26 and the SSP2, the damage almost doubles compared to the historical period, despite limited global warming. This increase is due to socioeconomic factors (see Figure 9). Figure 14 suggests that over the period 2070-2100, the representative concentration pathways RCP45 and RCP85 and *middle road* shared socioeconomic pathway (SSP2) lead respectively to global average annual damages 76% to 142% higher than in the

Figure 14: Global average annualized damage in SSPs (in billion USD)



RCP2.6, which is the concentration scenario allowing to maintain the global warming below 2°C. In addition, the relative proportions between RCPs are similar over SSPs. Table 1 shows that the whole distribution of damage over representative years is affected and simulated maximum values also increase sharply. In line with the wind distribution observed on Figure 7 on page 20, the distribution of damage is likely to expand, which is emphasized further by socio-economic factors.

Table 1: Simulated annualized damage statistics between 2070-2100 (in USD billion)

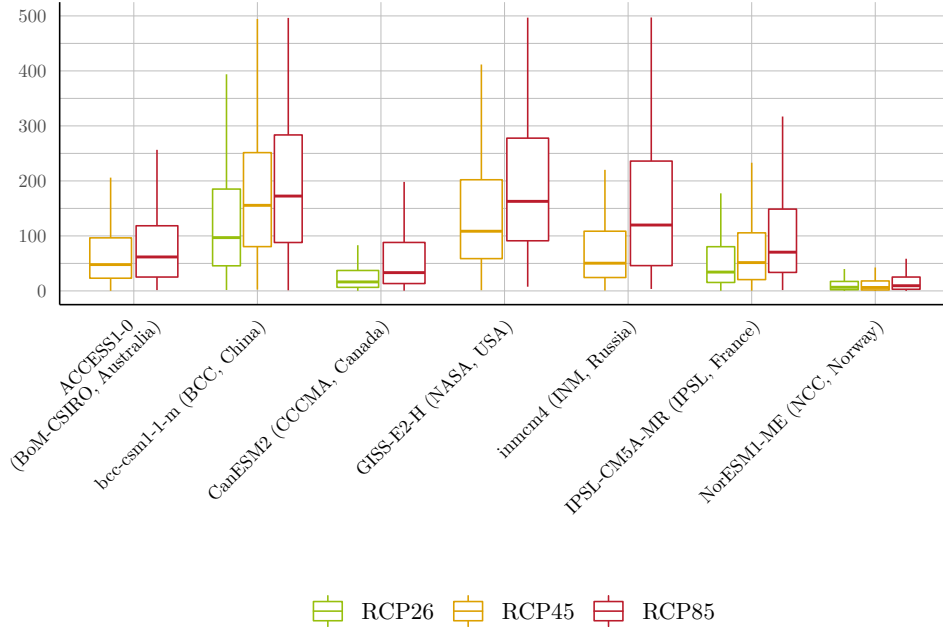
Climate conditions	Scenario	Mean	St. dev	Median	1st Qu.	3rd Qu.	99 th percentile	
1980-2000	Historical	53	34	44	35	57	146	
	RCP26	SSP2	76	144	29	9	84	468
		SSP3	52	96	21	7	59	305
		SSP4	57	121	18	5	58	379
		SSP5	136	269	45	15	144	895
RCP45	SSP2	134	210	68	22	166	727	
	SSP3	92	136	49	17	114	466	
	SSP4	98	172	43	13	112	599	
	SSP5	244	416	111	35	300	1388	
RCP85	SSP2	184	278	83	26	233	1013	
	SSP3	124	181	60	20	157	633	
	SSP4	136	227	53	16	166	792	
	SSP5	341	545	144	43	417	1975	

Table 1 shows the statistics of climate variability, i.e. distributions of damage obtained over the representative years simulated over the different concentration scenarios. Results reported in Table 1 are subject to many limitations and rely on multiple modeling assumptions. For instance, the physical asset value sensitivity to the projected GDP per capita growth

factor might not be linear and adaptation pathways will most likely strongly mitigate the expected damages in the SSP5. In addition, the grid resolution and physical exposure discrete aggregation technique could be improved by a precise dynamic modeling of the cyclone radius as in Bloemendaal *et al.* (2020). Wind fields could be introduced over geolocated asset maps using Holland (1980) similarly as in the CLIMADA module. However, the general framework is robust, and the proposed methodology could be generalized to any physical hazard, and geolocated assets after minor adjustments.

Another major source of uncertainty is the climate model used. The models produce substantially the same depression profiles on the historical period (see Figure 6) however they provide divergent projections of future climate. Figure 15 shows that different models produce highly different results. On this sample, it appears that the climate models BCC-CSM1-1-M and IPSL-CM5A-MR are the best suited to assess cyclone damages in concentration scenarios because of the availability of the data in each configuration and the consistency of the results with the historical period and the socioeconomic dynamics factors.

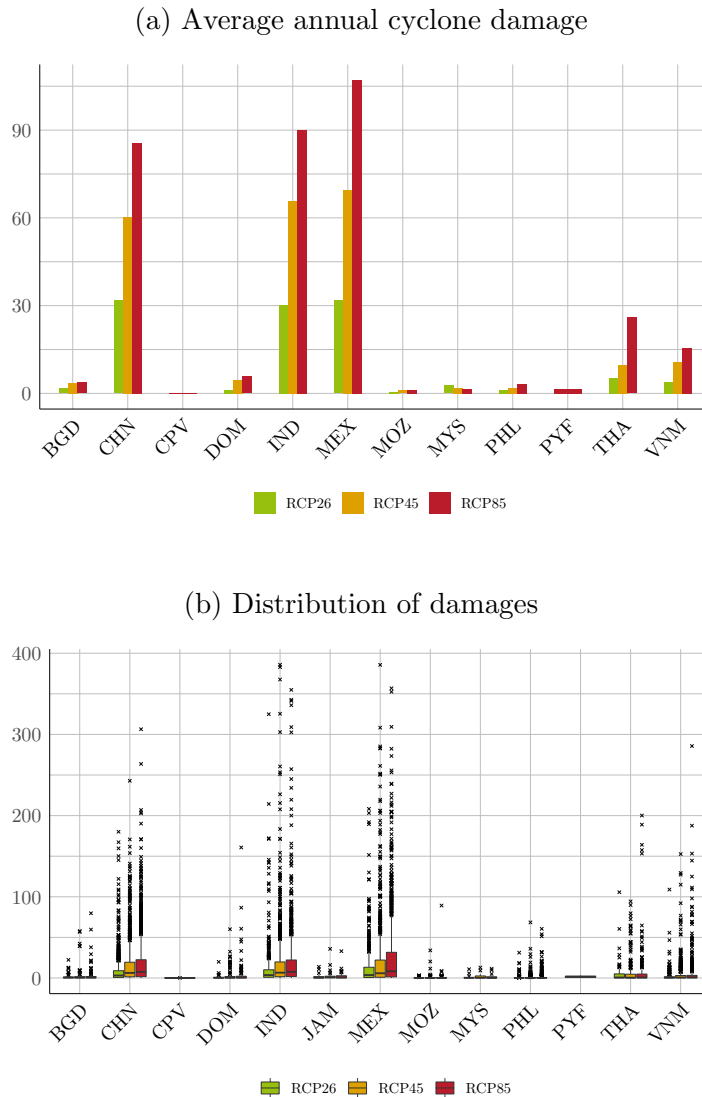
Figure 15: Climate models uncertainty in global average annualized damage simulation (billion USD). Each box is built on 250 representative years based on climate conditions projected on the period 2070-2100 by the corresponding climate models (except INM with 100 years).



At the country level, distinguishing damage sensitivity to climate change from other sources of uncertainty requires launching the model on a large number of representative years. The larger the country, the more accurate the assessment. For small countries, the model is sensitive to the occurrence of a cyclone landfall in the scenario simulated. Figure 16 shows the impact of climate change on a subset of emerging countries. Figure 16a presents

the average over each representative years, and Figure 16b presents the distributions of annualized cyclone-related damage in our simulations. The damages are similar regardless of the climate scenario for countries like the Philippines because of their high resiliency (see damage function WP2 on Figure 12), however we note a sharp increase in both average damage and outliers, i.e. extreme events. To conclude, at a country level, it appears clear that climate change has an effect on future annualized damage on average, but the real risk will most likely come from outliers increasingly frequent in higher concentration scenarios.

Figure 16: Example of emerging countries average damage (billion USD)



We use the SSP2 economic pathways results over all climate models. The annualized damage are averaged over more than 400 representative years in the RCP26, RCP45 and RCP85 between 2070 and 2100. In this Figure 16b we capped outliers at USD 400 billion for visualisation.

5 Impact of tropical cyclones on sovereign bond spreads under future climate conditions

In this section, we study the impact of cyclones on the exposed economies because of their higher vulnerability. A particular attention will be dedicated to emerging economies. We proceed in two steps. First we analyze how physical risks have affected the sovereign yields – bond returns and local currency valuation – of developing countries in the past. To this end, we study the behavior of financial variables around catastrophic events. In the second step, we use an econometric model to relate the spread of sovereign bonds to the scenario-based distributions of damage developed in Section 4.

5.1 Market integration of physical risks

Data To measure the impact of cyclones on the financial markets we extracted the bid prices of Treasury bonds (10 year and 3 months yields) and local currency valuation from Reuters Refinitiv and Bloomberg. We also tested the impact on 5 year credit default swaps (data source: Bloomberg). We use the dated disasters (when the start and end dates are known precisely) from EMDAT database⁶. To extend the database we use all types of natural disasters rather than just tropical storms. The database contains 496 dated events with costs above a USD 1 billion, 50 events with costs above USD 10 billion, 7 events with costs above USD 50 billion, and 2 events with costs above USD 100 billion from 1900 to 2021. Our aim is to quantify the impact of such events on financial markets, between 2000 and 2021.

Event study methodology Lanfear *et al.* (2019) showed that stock markets do respond to storm information using an event study approach. Recently, Dimov and Parsons (2021) analyzed the impact of historical cyclone landfall on the equity performance of manufacturers using a similar framework. From a sovereign perspective, in particular in emerging markets, low liquidity should mitigate market anticipation during cyclone formation (pre-landfall). The impact we seek to measure is the potential market meltdown after accounting for all the damages. Therefore, as a first approach to quantify the impact of natural catastrophes on sovereign markets, we perform an event study analysis on a 30 days window around the event end date, when total damage are observed. In absolute terms, for the given damage threshold value, for example USD 50 billion, we define the set of events affecting each country, in this case five events (see Figure 17). In relative terms, we normalized the events damage by the GDP of the country ($\mathcal{D}(t)/\text{GDP}$) and study the 100 most important events. For each event, we estimate abnormal the return it generates, using two approaches:

- With the constant mean approach, we compare the variation observed during the period with the averaged variation before the cyclone events:

$$\text{AR}_{j,t} = r_{j,t \in [\tau, \tau+w]} - \bar{r}_{j,t \in [\tau-w, \tau]} \quad (13)$$

where $\bar{r}_{j,t \in [\tau-w, \tau]}$ is the average variation of the variable of interest (for instance yields or currency variation) and $r_{j,t \in [\tau, \tau+w]}$ is the variation observed after the event.

⁶<https://public.emdat.be/data>.

- With the the market model approach, we compare the returns observed during the periods with the estimated returns of the financial security based on a CAPM-like model:

$$AR_{j,t} = r_{j,t \in [\tau, \tau+w]} - \widehat{\alpha}_{j,t \in [\tau-w, \tau]} - \widehat{\beta}_{j,t \in [\tau-w, \tau]} M_{r,t \in [\tau, \tau+w]} \quad (14)$$

where the r is the variation of market price variable (e.g. Treasury bonds price), $\widehat{\alpha}_{j,t \in [\tau-w, \tau]}$ and $\widehat{\beta}_{j,t \in [\tau-w, \tau]}$ are the coefficient of the CAPM model fitted on the period before the events and $M_{r,t \in [\tau, \tau+w]}$ is the time series of the market index variation after the event. Using a market model allows us to capture general fluctuations unrelated to country specific factors that can occur during the same period.

This methodology is very sensitive to the size of the estimation window and to the choice of the country. For yields or currency we will use the model based on constant mean correction (Equation 13). For bond price returns we will use the correction based on estimated returns (Equation 14), where the market returns are defined using 10 years U.S. bonds.

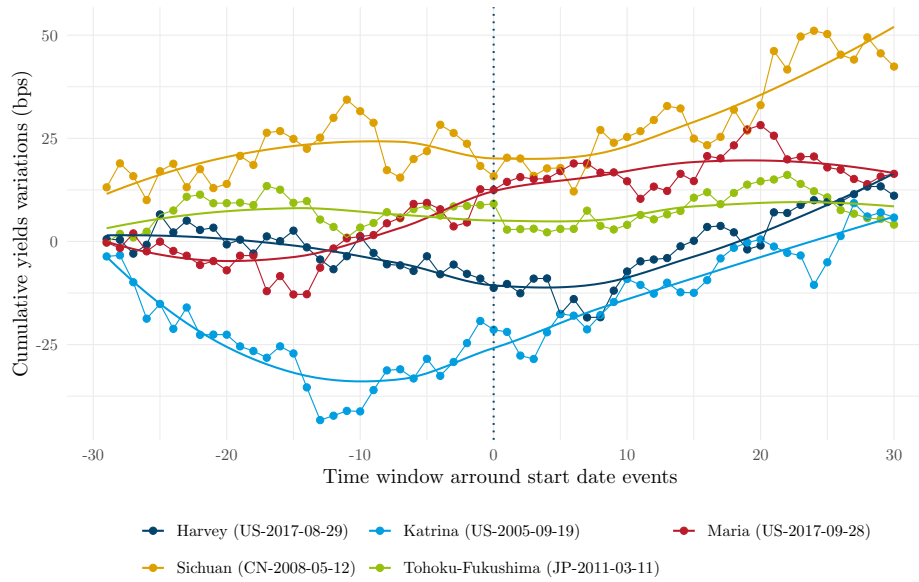
Impact on yields Over the 100 most damaging events relatively to the GDP of impacted countries, we find 55 matches with a series of daily 10 years yield variation suggesting an average 5 bps rise in emerging market bond yields (See Figure 20a on page 46). In absolute terms, the most extreme events are also the most impacting. For instance, considering dated events with cost over USD 50 billion restricts the database to the following five events: Tohoku, the Japanese earthquake and Tsunami (JP-2011-03-11) causing Fukushima, tropical cyclones Katrina (US-2005-09-19), Harvey (US-2017-08-29) and Maria (US-2017-09-28), and the Chinese Sichuan earthquake (CN-2008-05-12). The individual effects of these disasters on the cumulative variations of 10 year bond yields of the impacted countries are shown in Figure 17. This figure suggests that these events raised the cost of borrowing in the following months by 20 bps for affected countries⁷.

When restricting the database to the five most impacting events by normalizing the damage by the GDP of the country impacted we only keep Tohoku and Sichuan earthquakes, together with tropical cyclone Amphan (IN-2020-05-20), Thailand floods during the 2011 monsoon season (TH- 2011-08-05), or floods in India (IN-2019-09-30). Some catastrophic events – such as the floods in Pakistan (PK-2010-08-07) or cyclone Ivan passage through Cayman island (CY-2004-09-12) – could not be included because there are no matching yields in the database. However, there is no significant effect for the top five events and the results obtained using different filtering thresholds are not consistent.

Discussion The procedure described above was performed using several different financial variables: 10 year Treasury bond yield and market price, 3 months yield, currency valuation, and 5 year credit default swap. The results found for different instruments are not fully consistent with each other and depend on the parameters of the algorithm, therefore one cannot draw robust and general conclusions. However, all results suggest that in the past, emerging markets reacted to natural disaster by a slight depreciation of local currency, increase of bond yields and under-performance of the bonds. We also reiterate that the

⁷The aggregated impact are given Figure 20b.

Figure 17: Impact on 10 year sovereign yields



Top five most costly events. The event time is date end of the event reported by EMDAT the window is 30 days. The series are controlled using constant mean correction. Bid yield 10 years gov. from Reuters Refinitiv.

impact of disasters on more liquid stock markets was demonstrated (Lanfear *et al.*, 2019), therefore physical risks are already priced by the equity markets.

Although in the past, bond market reactions to catastrophic events have been moderate, climate change is increasing event intensity, which may lead to higher impact in the future. We showed that with the advent of climate change, annualized damages will grow and may compromise ability of some countries to pay back their debt. Therefore, in the next section we focus on default risk and investigate this question using the spread of their USD dominated bonds with respect to U.S. treasury bonds.

5.2 Cyclones impact on sovereign spreads

In this section, we derive the scenario-based excess spread for each country impacted by tropical cyclones.

From direct damage to the sovereign debt The first step is to define the transmission channels from the cyclone damage to the costs of sovereign debt. The damages related to disasters fall in two categories: the direct physical losses, possibly insured, and the longer-term economic consequences of the event. For instance, the direct costs of hurricane Katrina are estimated to USD 125 billion (2005), among which USD 80 billion were covered by insurance (EMDAT and Swiss Re Group (2020)). The consequences of the cyclone on the U.S. economic growth, which went down from 4.1% in the third quarter of 2005 to 1.7% in the fourth quarter before bouncing back to 5.4% in the first quarter of 2006, and on U.S. oil

production (19% of which was damaged)⁸ increased this cost further. It is sometimes hard to define long-term economic impact of the cyclone. For instance, cyclones often destroy agriculture and live stock, which affects the economy during a longer period. For instance, hurricanes Irma and Maria in 2017 in Dominica destroyed 100% of agricultural plantations, while Yassi in Australia in 2011 destroyed 75% of agricultural plantations in the affected areas.

In general, because of the propagation of damages in the economic system, the longer-term economic impacts are more complex to estimate. To address this difficulty, Hallegatte (2008) introduced an input-output framework and defined the economic amplification ratio (EAR) as the multiplier between direct cost and the total economic damage. For Katrina this coefficient was estimated to be 1.39. The author suggested that the economic outcomes of events with direct losses exceeding USD 200 billion could imply total cost twice as large. In this case, the increase of the cost because of climate change (cf. Table 1) may overwhelm reconstruction capacity of poorest countries. In our estimation we do not apply an economic amplification ratio because we consider that the damage reported already takes this effect into account.

In this section, we develop a simplified approach for assessing the effect of cyclone damage on sovereign credit spread, assuming that the cost of damages is paid by issuing new government debt. We build a structural econometric model for sovereign spread, including the debt to GDP ratio as an explanatory variable (Hilscher & Nosbusch, 2010). Assuming stationarity of model parameters then allows us to evaluate the effect of cyclone damages on spreads under various climate and economic scenarios.

Sovereign spread model The spread is the difference of yield between a given security and the risk-free asset i.e. AAA rated bond. In practice, we use the option-adjusted spread with respect to the U.S. 10 year Treasury bond. The option-adjusted spread (OAS) is the measurement of the spread adjusted to take into account specific options embedded in some fixed-income securities. Following Hilscher and Nosbusch (2010), we calibrate a cross-sectional econometric model for the option-adjusted spread based on annual end-of-year data:

$$\begin{aligned} \text{OAS}_t = \alpha &+ \beta_1 \Delta \mathcal{C}_t + \beta_2 D_t + \beta_3 \text{VIX}_t + \beta_4 r_t^{10Y} \\ &+ \beta_5 \text{TED}_t + \beta_6 \frac{L_t}{\text{GDP}_t} + \beta_7 \frac{\text{reserves}_t}{\text{GDP}_t} + \beta_8 \mathcal{R}_t + \beta_9 \mathcal{K}_t + \varepsilon_t. \end{aligned} \quad (15)$$

OAS is the end-of-year option adjusted spread, from from JP Morgan EMBI position report in BarraOne;

\mathcal{C} is the commodity price index, from Reuters Refinitiv;

D is the average duration of the bonds, from JP Morgan EMBI position report in BarraOne;

VIX is the CBOE volatility index, from Reuters Refinitiv;

⁸<https://www.thebalance.com/hurricane-katrina-facts-damage-and-economic-effects-3306023>.

r^{10Y} is the 10 year U.S. Treasury bonds rate, from Reuters Refinitiv;

TED is the difference between the three-month Treasury bill and the three-month LIBOR, from Reuters Refinitiv;

L refers to the total external debt stocks in USD, from World Bank;

GDP refers to the end-of-year GDP, from World Bank;

reserves are the total reserves including gold, in USD;

\mathcal{R} is the credit rating dummy variable (described below);

\mathcal{K} is the country dummy variable, described below.

The model covers 74 countries between 2010 and 2020.

We chose to use all the bonds constituting the index, i.e. including multiple bonds per country per date. Rather than using Hilscher and Nosbusch (2010) fixed effect approach with our unbalanced panel, we chose to fit a simple ordinary least squares regression including dummies for ratings and country effects. Table 2 shows the sensitivity of the option adjusted spread of each bond belonging to the JP Morgan EMBI to macroeconomic and financial factors following Hilscher and Nosbusch (2010). The model (1) assesses the effect of a variation of debt/GDP ratio only, the model (2) introduces one rating dummy (splitting below B-), the model (3) introduces additional macro variables and (4) adds country effect dummies and bond duration⁹.

In line with Edwards (1986), we find that the debt ratio is significant. More importantly, we note that β_6 is relatively stable over the modeling frameworks implying that the sensitivity of the spread to a sudden increase of debt ratio does not strongly depend on external nor idiosyncratic parameters. We find a positive effect of the VIX, and a hardly significant effect from TED spread. The duration of the bonds is of the expected sign and significant. The U.S. 10 years return has a negative effect on emerging country spread. This could be linked to two reasons. First, when the U.S. bond yield increases, investors may be less interested in emerging markets. Another reason is the positive correlation between Treasury returns and the dollar index¹⁰, and negative correlation between the dollar index and emerging markets debt. In other words, the USD denominated debt of these countries grows when their local currency depreciates. Most of these countries are commodity exporters. A positive change in commodity price index, implies that a country's exports have become more expensive relative to its imports (Hilscher & Nosbusch, 2010). Therefore, we expect commodity price index to reduce sovereign spreads. This is an important channel of diffusion of the risks towards developing countries less exposed to tropical cyclones. The coefficients of models (3) and (4) are of the expected sign. Including country effects in (4) we obtain a model reaching 71.5% of adjusted R².

⁹Including bond duration is significant only when controlling by country effect.

¹⁰The U.S. Dollar Index (USDIX) is an index of the value of the United States dollar relative to a basket of foreign currencies.

Table 2: Simple Option-Adjusted-Spread model

	<i>Dependent variable:</i>			
	OAS (bp)			
	(1)	(2)	(3)	(4)
ΔC_T			-486.681*** (114.675)	-467.219*** (91.876)
Duration				8.639*** (1.659)
VIX			17.094*** (2.510)	15.377*** (2.120)
TED			-13.753 (113.318)	-7.395 (91.791)
rUS,10Y			-9.800*** (2.199)	-8.478*** (1.756)
$\frac{L}{GDP}$	367.461*** (26.060)	229.629*** (21.319)	336.718*** (25.809)	377.035*** (79.759)
$\frac{\text{reserves}}{GDP}$			-244.949*** (41.034)	-1,176.650*** (185.851)
Rating <B-		1,692.843*** (42.121)	1,697.096*** (41.011)	1,391.009*** (36.858)
Countries				X
Constant	207.254*** (15.583)	222.600*** (12.732)	1,410.488*** (330.158)	1,521.181*** (269.092)
Observations	2,212	1,860	1,832	1,832
R ²	0.083	0.509	0.542	0.723
Adjusted R ²	0.082	0.509	0.541	0.715
Residual Std. Error	411.571 (df = 2210)	316.591 (df = 1857)	308.258 (df = 1824)	242.855 (df = 1778)
F Statistic	198.832*** (df = 1; 2210)	962.874*** (df = 2; 1857)	308.792*** (df = 7; 1824)	87.609*** (df = 53; 1778)

Note: Dropping Argentina in constant in (4) *p<0.1; **p<0.05; ***p<0.01

Cyclone impact on sovereign spreads under representative concentration pathways We now use the econometric model developed in the previous paragraph to assess the impact of tropical cyclones on emerging country bond spreads under relative concentration pathways. To this end, we make the following simplifying assumptions:

- We assume that the bond spread model parameters remain stable over time;
- We assume that the cyclone damages are financed directly by the government by issuing new debt, and that other variables of the model are not affected by cyclones;
- We take into account only direct impact of cyclones and not the total economic costs.

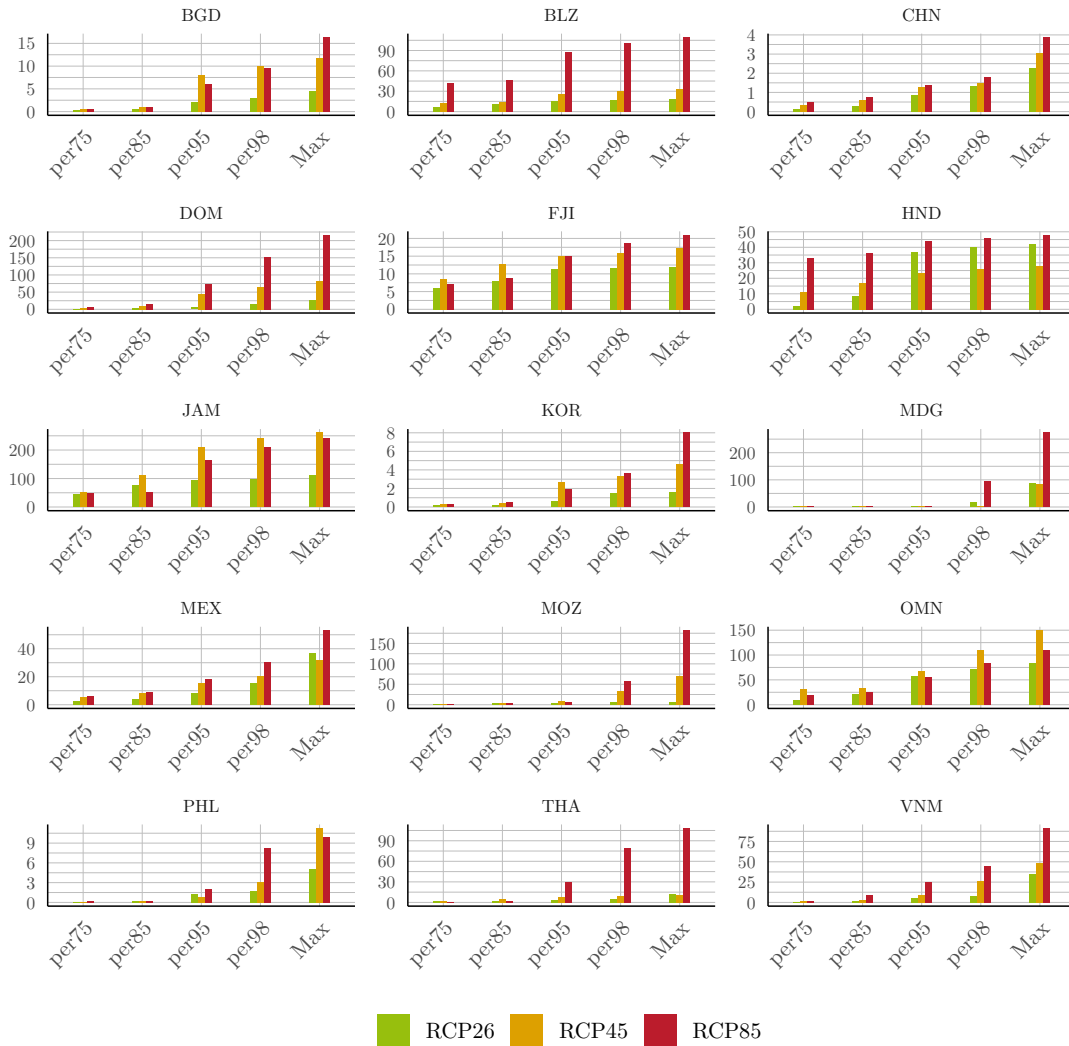
For each country j in the JP Morgan EMBI index, we assess the annual bond spread variation due to cyclone damage, in scenario k for the year t using the following formula:

$$\Delta_{k,t} \text{OAS}(j, k, t) = \beta_6 \times \frac{\mathcal{D}(j, k, t)}{F_{\text{GDP}}(j, k, t) \text{GDP}(j, 2020)}, \quad (16)$$

where we recall that \mathcal{D} stands for annualized cyclone damage, and F_{GDP} is the GDP growth factor for the specified country/scenario.

We compare the spread variation defined from damages of the RCP26 baseline, RCP45 and RCP85 to obtain an annualized financial valuation of the cyclone-related physical climate

Figure 18: Damage cost channeled to excess spread in emerging countries



risk. In terms of average spread variation on larger emerging countries, we observe little effect of climate change on the spread of issued securities channeled by the impact on debt-to-GDP ratio. Ignoring outliers, i.e. focusing on the part of the distribution between 25% and 75% quantiles, annualized damage has limited impact on individual countries¹¹. This is consistent with the historical data, as countries are not equally affected each year by tropical cyclones, and when they are, they develop a resiliency that is reflected in their damage functions. Therefore, we focused on the extreme event quantiles. Figure 18 represents the excess cyclone-related spread for a sample of countries for the 75th, 85th, 95th, 98th percentile and the maximum cyclone related shock observed in the simulations. In this sample, larger countries excess spreads remain limited (without economic amplification factors). However, these simulations suggest that the most vulnerable countries in the Caribbean basin are

¹¹This would be to exclude the events studied in Figure 17 for instance.

clearly exposed to spread increase (up to 200 bps) in case of extreme storm making landfall in the highest concentration scenarios. One needs to keep in mind that our model assumes a linear relationship between debt to GDP ratio and bond spread which may not hold for such extreme damages, which may totally overwhelm the reconstruction capacity of the countries and lead to their default.

6 Conclusion

This paper proposes a structural framework for assessing the impact of tropical cyclones on sovereign spreads. We first present a methodology to generate synthetic storms based on large-scale climate data and show that when used with reanalysis data, our method produces tracks consistent with historical observations. We then use our method with CMIP5 model projections and show that climate change will increase the intensity and frequency of extreme events. In particular, the maximum wind speeds will increase in the RCP45 and RCP85 by respectively 9.5% and 13.5% by 2070-2100. These synthetic tracks have several applications. The first one is in natural disaster risk management, to calibrate adaptation measures. For this purpose, the track generation algorithm may be enhanced, for instance, by including dependency in the latitudinal and longitudinal incremental displacement, coupling with meteorological forecasting model, or including ground topography to model the cyclone displacement over land. Another major field of application is to climate financial risk management, where this scenario-based events database can be used to price physical risk by constructing risk density maps to compute portfolio exposure. This would require to better define asset-level vulnerabilities.

In the second main section of this paper, we introduce multiple datasets to define and project sovereign physical asset at risk. In practice, this step can be substituted by corporate geolocated asset and supply chain data in order to adapt this framework to stress companies sensitivity to cyclone risks. Concomitantly, the damage functions must be defined and calibrated so the results can be compared with respect to a plausible baseline scenario. The main pitfall of this section is the data mining step required to properly calibrate the functions, which is, despite the regional specification, the major source of uncertainty (see Figure 8a in Supplementary Material showing the distribution of plausible functions in the U.S.). Nevertheless, it is possible to calibrate the model such as the aggregated results are consistent with the historical records. This section's results suggest that over the period 2070-2100, the representative concentration pathways RCP45 and RCP85 and *middle road* shared socioeconomic pathway (SSP2) lead respectively to global average annual damages 76% to 142% higher than in the RCP2.6, concentration scenario allowing to maintain the global warming below 2°C. Barro (2006) and Barro and Ursúa (2012) showed that rare disasters were more impacting for the financial markets. Thus, climate change really represents a significant risk as it lowers the frequency and sharply increases the disaster intensity.

In the last section, we focus on ways to measure extreme event impact on financial markets. We performed an event study to measure market reaction during the time windows around the events. Because of the small number of events, data quality issues and low liquidity of sovereign emerging markets securities, we can hardly draw robust conclusions from this backward looking exercise. It appears that some financial variables react to cyclones

damages but the results are too sensitive to parameters. Next, we explore the transmission channel of the scenario-based damage to JP Morgan EMBI sovereign bond spread by assuming that cyclone damage costs are financed by issuing extra external debt. Following Hilscher and Nosbusch (2010), we build a simple econometric model for the bond spread, and quantify the excess spread generated by cyclones assuming that there is no economic amplification ratio. We show that the maximum annual cyclone-related spread change for most vulnerable emerging countries can increase up to 200bps under future climate scenarios.

As all long-term economic projections, our results are subject to multiple sources of uncertainty, including climate uncertainty, model uncertainty, damage function uncertainty as well as different socio-economic uncertainties. Some of these uncertainties are quantified in the paper using Monte Carlo simulation with different RCP scenarios, different SSP pathways, and a variety of climate models.

References

- AUFFHAMMER, M. (2018). *Quantifying economic damages from climate change*. *Journal of Economic Perspectives*, 32(4), 33–52.
- AZNAR SIGUAN, G., & BRESCH, D. N. (2019). *CLIMADA v1: a global weather and climate risk assessment platform*. *Geoscientific Model Development*, 12, 3085–3097.
- BACMEISTER, J. T., REED, K. A., HANNAY, C., LAWRENCE, P., BATES, S., TRUESDALE, J. E., ROSENBLUM, N., & LEVY, M. (2018). *Projected changes in tropical cyclone activity under future warming scenarios using a high-resolution climate model*. *Climatic Change*, 146(3-4), 547–560.
- BANTWAL, V. J., & KUNREUTHER, H. C. (2000). *A cat bond premium puzzle? The Journal of Psychology and Financial Markets*, 1(1), 76–91.
- BARRO, R. J. (2006). *Rare disasters and asset markets in the twentieth century*. *The Quarterly Journal of Economics*, 121(3), 823–866.
- BARRO, R. J., & URSÚA, J. F. (2012). *Rare macroeconomic disasters*. *Annu. Rev. Econ.*, 4(1), 83–109.
- BATTISTON, S., MANDEL, A., MONASTEROLO, I., SCHÜTZE, F., & VISENTIN, G. (2017). *A climate stress-test of the financial system*. *Nature Climate Change*, 7(4), 283–288.
- BATTISTON, S., & MONASTEROLO, I. (2019). *A climate risk assessment of sovereign bonds' portfolio*. *University of Milan Bicocca Department of Economics, Management and Statistics Working Paper*, (420).
- BEIRNE, J., RENZHI, N., & VOLZ, U. (2020). *Feeling the heat: Climate risks and the cost of sovereign borrowing*.
- BLOEMENDAAL, N., HAIGH, I. D., de MOEL, H., MUIS, S., HAARSMA, R. J., & AERTS, J. C. (2020). *Generation of a global synthetic tropical cyclone hazard dataset using STORM*. *Scientific Data*, 7(1), 1–12.
- BRESCH, D. N. (2017). *CLIMADA-the open-source and-access global probabilistic risk modelling platform*.
- BUTCHART, N., AUSTIN, J., KNIGHT, J. R., SCAIFE, A. A., & GALLANI, M. L. (2000). *The response of the stratospheric climate to projected changes in the concentrations*

- of well-mixed greenhouse gases from 1992 to 2051. *Journal of climate*, 13(13), 2142–2159.
- CARNEY, M. (2015). *Breaking the Tragedy of the Horizon—climate change and financial stability. Speech given at Lloyd’s of London, 29*, 220–230.
- CHAVAS, D. R., REED, K. A., & KNAFF, J. A. (2017). *Physical understanding of the tropical cyclone wind-pressure relationship. Nature communications*, 8(1), 1–11.
- DEMARIA, M., & KAPLAN, J. (1994). *A statistical hurricane intensity prediction scheme (SHIPS) for the Atlantic basin. Weather and Forecasting*, 9(2), 209–220.
- DEMARIA, M., KNAFF, J. A., & CONNELL, B. H. (2001). *A tropical cyclone genesis parameter for the tropical Atlantic. Weather and Forecasting*, 16(2), 219–233.
- DIMOV, I., & PARSONS, T. (2021). *Quantifying the impact of cyclones on equity returns of manufacturers. Bloomberg whitepaper*.
- EATON, J., & GERSOVITZ, M. (1981). *Debt with potential repudiation: Theoretical and empirical analysis. The Review of Economic Studies*, 48(2), 289–309.
- EBERENZ, S., LÜTHI, S., & BRESCH, D. N. (2020). *Regional tropical cyclone impact functions for globally consistent risk assessments. Natural Hazards and Earth System Sciences Discussions*, 1–29.
- EBERENZ, S., STOCKER, D., RÖÖSLI, T., & BRESCH, D. N. (2019). *LitPop: Global Exposure Data for Disaster Risk Assessment*.
- EBERENZ, S., STOCKER, D., RÖÖSLI, T., & BRESCH, D. N. (2020). *Asset exposure data for global physical risk assessment. Erath Syst*, 12. <https://doi.org/10.5194/essd-12-817-2020>
- EDWARDS, S. (1986). *The pricing of bonds and bank loans in international markets: An empirical analysis of developing countries’ foreign borrowing. European Economic Review*, 30(3), 565–589.
- ELSNER, J. B., KOSSIN, J. P., & JAGGER, T. H. (2008). *The increasing intensity of the strongest tropical cyclones. Nature*, 455(7209), 92–95.
- EMANUEL. (1988). *The maximum intensity of hurricanes. Journal of the Atmospheric Sciences*, 45(7), 1143–1155.
- EMANUEL. (1991). *The theory of hurricanes. Annual Review of Fluid Mechanics*, 23(1), 179–196.
- EMANUEL. (1999). *Thermodynamic control of hurricane intensity. Nature*, 401(6754), 665–669.
- EMANUEL. (2005). *Increasing destructiveness of tropical cyclones over the past 30 years. Nature*, 436(7051), 686–688.
- EMANUEL. (2011). *Global warming effects on US hurricane damage. Weather, Climate, and Society*, 3(4), 261–268.
- EMANUEL, K., SUNDARARAJAN, R., & WILLIAMS, J. (2008). *Hurricanes and global warming: Results from downscaling IPCC AR4 simulations. Bulletin of the American Meteorological Society*, 89(3), 347–368.
- FORSTER, P. M., BODEKER, G., SCHOFIELD, R., SOLOMON, S., & THOMPSON, D. (2007). *Effects of ozone cooling in the tropical lower stratosphere and upper troposphere. Geophysical Research Letters*, 34(23).

- GAO, J. (2020). *Downscaling global spatial population projections from 1/8-degree to 1-km grid cells. Technical Notes NCAR, National Center for Atmospheric Research, Boulder, CO., USA.* <https://doi.org/10.7927/q7z9-9r69>
- GRAY, W. M. (1975). *Tropical cyclone genesis. Atmospheric science paper; no. 234.*
- GUHA-SAPIR, D., BELOW, R., & HOYOIS, P. (2018). *EM-DAT: the CRED/OFDA international disaster database.*
- HALLEGATTE, S. (2008). *An adaptive regional input-output model and its application to the assessment of the economic cost of Katrina. Risk Analysis: An International Journal, 28(3), 779–799.*
- HILSCHER, J., & NOSBUSCH, Y. (2010). *Determinants of sovereign risk: Macroeconomic fundamentals and the pricing of sovereign debt. Review of Finance, 14(2), 235–262.*
- HOLLAND, G. J. (1980). *An analytic model of the wind and pressure profiles in hurricanes. Monthly weather review, 108(8), 1212–1218.*
- HOLLAND, G. J. (1997). *The maximum potential intensity of tropical cyclones. Journal of the atmospheric sciences, 54(21), 2519–2541.*
- JAMES, M., & MASON, L. (2005). *Synthetic tropical cyclone database. Journal of waterway, port, coastal, and ocean engineering, 131(4), 181–192.*
- JAMES, M., & MASON, L. (2006). *Closure to “Synthetic Tropical Cyclone Database” by MK James and LB Mason. Journal of Waterway, Port, Coastal, and Ocean Engineering, 132(6), 502–503.*
- JEWELL, J., & CHERP, A. (2020). *On the political feasibility of climate change mitigation pathways: Is it too late to keep warming below 1.5° C? Wiley Interdisciplinary Reviews: Climate Change, 11(1), e621.*
- JONES, B., & O’NEILL, B. C. (2020). *Global One-Eighth Degree Population Base Year and Projection Grids Based on the Shared Socioeconomic Pathways. Palisades, (Revision 01).* <https://doi.org/10.7927/m30p-j498>
- KAPLAN, J., & DEMARIA, M. (1995). *A simple empirical model for predicting the decay of tropical cyclone winds after landfall. Journal of applied meteorology, 34(11), 2499–2512.*
- KLUSAK, P., AGARWALA, M., BURKE, M., KRAEMER, M., & MOHADDES, K. (2021). *Rising Temperatures, Falling Ratings: The Effect of Climate Change on Sovereign Creditworthiness.* Faculty of Economics, University of Cambridge.
- KNAFF, J. A., & ZEHR, R. M. (2007). *Reexamination of tropical cyclone wind–pressure relationships. Weather and Forecasting, 22(1), 71–88.*
- KNAPP, K. R., KRUK, M. C., LEVINSON, D. H., DIAMOND, H. J., & NEUMANN, C. J. (2010). *The international best track archive for climate stewardship (IBTrACS) unifying tropical cyclone data. Bulletin of the American Meteorological Society, 91(3), 363–376.*
- KNUTSON, T. R., MCBRIDE, J. L., CHAN, J., EMANUEL, K., HOLLAND, G., LANDSEA, C., HELD, I., KOSSIN, J. P., SRIVASTAVA, A., & SUGI, M. (2010). *Tropical cyclones and climate change. Nature geoscience, 3(3), 157–163.*
- KOSSIN, J. P., KNAPP, K. R., OLANDER, T. L., & VELDEN, C. S. (2020). *Global increase in major tropical cyclone exceedance probability over the past four decades. Proceedings of the National Academy of Sciences, 117(22), 11975–11980.*

- LANFEAR, M. G., LIOUI, A., & SIEBERT, M. G. (2019). *Market anomalies and disaster risk: Evidence from extreme weather events*. *Journal of Financial Markets*, 46, 100477.
- LÜTHI, S. (2019). *Applying Machine Learning Methods to the Assessment of Tropical Cyclone Impacts*.
- MALLUCCI, E. (2020). *Natural Disasters, Climate Change, and Sovereign Risk*. *International Finance Discussion Papers 1291*.
- MENDELSON, R., EMANUEL, K., CHONABAYASHI, S., & BAKKENSEN, L. (2012). *The impact of climate change on global tropical cyclone damage*. *Nature climate change*, 2(3), 205–209.
- MORANA, C., & SBRANA, G. (2019). *Climate change implications for the catastrophe bonds market: An empirical analysis*. *Economic Modelling*, 81, 274–294.
- NEU, U., AKPEROV, M. G., BELLENBAUM, N., BENESTAD, R., BLENDER, R., CABALLERO, R., COCOZZA, A., DACRE, H. F., FENG, Y., FRAEDRICH, K., et al. (2013). *IMILAST: A community effort to intercompare extratropical cyclone detection and tracking algorithms*. *Bulletin of the American Meteorological Society*, 94(4), 529–547.
- NORDHAUS, W. D. (1993). *Optimal greenhouse-gas reductions and tax policy in the "DICE" model*. *The American Economic Review*, 83(2), 313–317.
- NOY, I. (2016). *The socio-economics of cyclones*. *Nature Climate Change*, 6(4), 343–345.
- PACHAURI, R. K., ALLEN, M. R., BARROS, V. R., BROOME, J., CRAMER, W., CHRIST, R., CHURCH, J. A., CLARKE, L., DAHE, Q., DASGUPTA, P., et al. (2014). *Climate Change 2014: Synthesis Report. Contribution Of Working Groups I, II And III To The Fifth Assessment Report Of The Intergovernmental Panel On Climate Change*. Ipc.
- PIELKE JR, R. A., GRATZ, J., LANDSEA, C. W., COLLINS, D., SAUNDERS, M. A., & MUSULIN, R. (2008). *Normalized hurricane damage in the United States: 1900–2005*. *Natural Hazards Review*, 9(1), 29–42.
- PINDYCK, R. S. (2017). *The use and misuse of models for climate policy*. *Review of Environmental Economics and Policy*, 11(1), 100–114.
- PINTO, J. G., KARREMANN, M. K., BORN, K., DELLA-MARTA, P. M., & KLAWA, M. (2012). *Loss potentials associated with European windstorms under future climate conditions*. *Climate Research*, 54(1), 1–20.
- PRAHL, B. F., RYBSKI, D., BOETTLE, M., & KROPP, J. P. (2016). *Damage functions for climate-related hazards: unification and uncertainty analysis*. *Natural Hazards and Earth System Sciences*, 16(5), 1189–1203.
- PRAHL, B. F., RYBSKI, D., BURGHOFF, O., & KROPP, J. P. (2019). *Comparison of storm damage functions and their performance*.
- RAMASWAMY, V., SCHWARZKOPF, M., RANDEL, W., SANTER, B., SODEN, B. J., & STENCHIKOV, G. (2006). *Anthropogenic and natural influences in the evolution of lower stratospheric cooling*. *Science*, 311(5764), 1138–1141.
- RIAHI, K., van VUUREN, D. P., KRIEGLER, E., EDMONDS, J., O'NEILL, B. C., FUJIMORI, S., BAUER, N., CALVIN, K., DELLINK, R., FRICKO, O., LUTZ, W., POPP, A., CUARESMA, J. C., KC, S., LEIMBACH, M., JIANG, L., KRAM, T., RAO, S., EMERLING, J., ... TAVONI, M. (2017). *The Shared Socioeconomic Pathways and their*

- energy, land use, and greenhouse gas emissions implications: An overview. Global Environmental Change, 42*, 153–168. <https://doi.org/10.1016/j.gloenvcha.2016.05.009>
- SOLOMON, S., MANNING, M., MARQUIS, M., QIN, D., et al. (2007). *Climate Change 2007-the Physical Science Basis: Working Group I Contribution To The Fourth Assessment Report Of The IPCC*. Cambridge university press.
- SWISS RE GROUP. (2020). *Ten Years After Katrina*.
- TAYLOR, K. E., STOUFFER, R. J., & MEEHL, G. A. (2012). *An overview of CMIP5 and the experiment design. Bulletin of the American meteorological Society, 93*(4), 485–498.
- TIMMERMANN, A., CHU, J.-E., LEE, S.-S., WENGEL, C., STUECKER, M. F., & YAMAGUCHI, R. (2020). *Tropical cyclone response to anthropogenic warming as simulated by a mesoscale-resolving global coupled earth system model*.
- VOLZ, U., BEIRNE, J., AMBROSIO PREUDHOMME, N., FENTON, A., MAZZACURATI, E., RENZHI, N., & STAMPE, J. (2020). *Climate change and sovereign risk*.
- WEINKLE, J., LANDSEA, C., COLLINS, D., MUSULIN, R., CROMPTON, R. P., KLOTZBACH, P. J., & PIELKE, R. (2018). *Normalized hurricane damage in the continental United States 1900–2017. Nature Sustainability, 1*(12), 808–813.
- WEINKLE, J., MAUE, R., & PIELKE JR, R. (2012). *Historical global tropical cyclone landfalls. Journal of Climate, 25*(13), 4729–4735.
- WEITZMAN, M. L. (2010). *What Is The "Damages Function" For Global Warming—And What Difference Might It Make? Climate Change Economics, 1*(01), 57–69.
- YE, M., WU, J., LIU, W., HE, X., & WANG, C. (2020). *Dependence of tropical cyclone damage on maximum wind speed and socioeconomic factors. Environmental Research Letters, 15*(9), 094061.
- ZARZYCKI, C. M., REED, K. A., BACMEISTER, J. T., CRAIG, A. P., BATES, S. C., & ROSEN-BLOOM, N. A. (2016). *Impact of surface coupling grids on tropical cyclone extremes in high-resolution atmospheric simulations. Geoscientific Model Development (Online), 9*(2).

A Notation

		Indices
B	Basin	
i	Cyclone	
j	Country (or region)	
k	Scenario	
s	Generative algorithm step $s \sim (x, y, t)$	
t	Date	
s_l, t_L	Step on land	
x	Longitude	
y	Latitude	
env	Environmental standard season/location variable	
		Variables
\mathcal{C}	is the commodity price index	
D	Bond duration land	
$D^l(x_t, y_t, t)$	Distance to land	km
$\mathcal{D}(j, k, t)$	Simulated cyclone annualized damage	USD
$f(y)$	Coriolis parameter ($2\omega \sin(y)$)	
f_j	Fraction damage ratio	
$F_{pop}(x, y, k, t)$	Population variation (local level)	
$F_{GDP}(j, k, t)$	GDP variation (country level)	
$F_{GDP}^{cap}(j, k, t)$	GDP per capita (country level)	
$GDP(j, k, t)$	Global Domestic Product	USD
$\mathcal{L}(x, y)$	Local physical asset value	USD
$L(j, k, t)$	Total debt (external)	USD
$MSLP(x_t, y_t, t)$	Mean sea surface pressure	Pa (or hPa)
$MPD(SST_b)$	Max pressure drop observed for a given SST	Pa (or hPa)
OAS	option adjusted spread	pbs
P_t^c	Central pressure	Pa (or hPa)
$P(j, k, t)$	Population (country level)	number of people
$p(x, y, t)$	local population estimate	number of people
$q(x_t, y_t, t)$	Specific humidity	
$r_{env}(i, t)$	Radius to environmental conditions	km
$RH(x_t, y_t, t)$	Relative humidity	%
SED_i	Simulated damage per cyclone	USD
$SST(x_t, y_t, t)$	Sea surface temperature	K
SST_b	Temperature rounded to 0.1°C	K
$T_{\text{tropo}}(x_t, y_t, t)$	Tropopause temperature	K
V_t	Wind speed	m/s
$\Phi_c(i, j, k, t)$	Sovereign physical asset exposure	USD
x_t	Longitude along track	
y_t	Latitude along track	

Pricing Cyclone-Related Physical Risk

Functions and operators	
Δ_t	Variation over time operator ($X(t)/X(t-1)$)
Δ_k	Variation over scenario operator ($X(k)/X(k=0)$)
Parameter	
a, b	Wind-pressure relationship coefficients
A, B, C	SST-MPD coefficients
a_n	AR longitude parameters
b_n	AR latitude parameters
c_n	Dynamic pressure variation
μ_X	Mean of the normal distribution fitted on variable X
d_n	Physical damage parameters
R_d	Dry air constant
t_0	Year 2020
L_v	Latent heat constant
ρ	Surface air density
σ_X	Standard deviation of the normal distribution fitted on variable X
v_t	Wind threshold (25.7m/s)
v_h	Wind function hyper parameter calibrated

B Complementary materials

Algorithm 1: Cyclone Track Generator

Result: Definition of each cyclone trajectory and properties

$$\begin{aligned}
 V(s=0) &= 20 \text{ m/s} \\
 \text{MSLP} - P_c(s=0) &= \left(\frac{V}{a}\right)^{1/b} \propto \text{Equation (3)} \\
 &\sim 25 \text{ hPa} \\
 P_c(s=0) &\sim 990 \text{ hPa}
 \end{aligned}$$

while $\text{MSLP} - P_c > 0$ $\&\&$ $V > v_m$ **do**

 Extract $D(s)$ from naturalearth coastlines;

$$x(s) = x(s-1) + \Delta x(s) + \mathcal{N}(\mu_{x,B}, \sigma_{x,B})$$

 where $\Delta x(s) \propto \text{Equation (1)}$

$$y(s) = y(s-1) + \Delta y(s) + \mathcal{N}(\mu_{y,B}, \sigma_{y,B})$$

 where $\Delta y_t \propto \text{Equation (2)}$

$$\text{MPI}(s) = f_{\text{MPI}}(y(s), P_c(s-1), \text{SST}(s), T_{\text{tropo}}(s), \text{MSLP}(s), \text{RH}(s))$$

$f_{\text{MPI}} \propto \text{Equation (4)}$

$$P_c(s) = \max(P_c(s) + \Delta P_c(s), \text{MSLP}(s) - \text{MPD}(s))$$

$\text{MPD} \propto \text{Equation (5)}$ $\&$

$\Delta P_c(s) \propto \text{Equation (6)}$

$$V(s) = a(\text{MSLP} - P_c(s))^b$$

if *on land* = TRUE **then**

 | $s_l = s_l + 1$

end

if $s_l > 4$ **then**

 Compute distance to land $D(s)$ from naturalearth coastlines;

$$V(s) = V_b + (R \cdot V_0 - V_b)e^{-\alpha s_l} - m(t_L) \left(\ln \frac{D}{D_0} \right) + b(t_L)$$

$V(s) \propto \text{Equation (7)}$

end

end

Figure 19: Regional F_{cap} factor variation in SSPs IIASA database

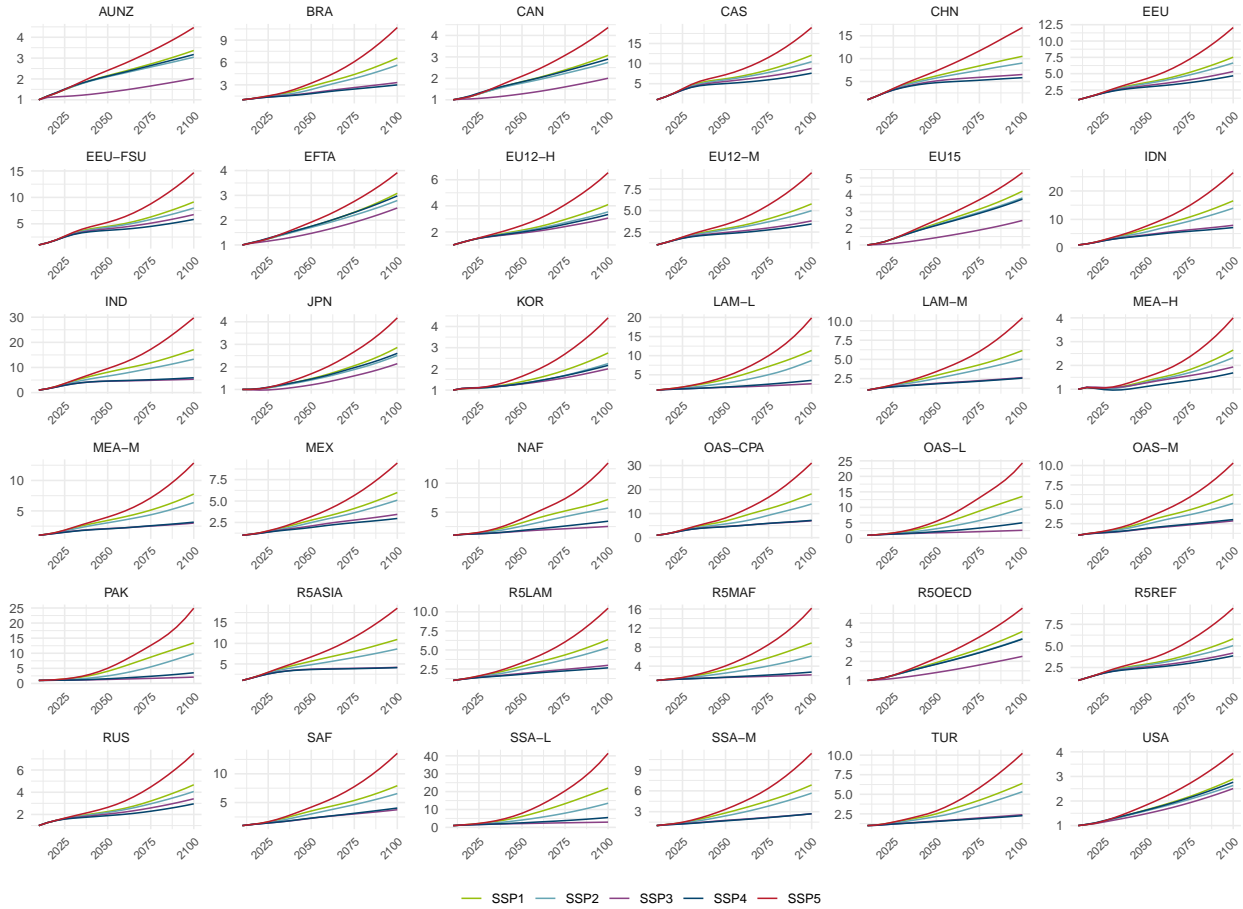
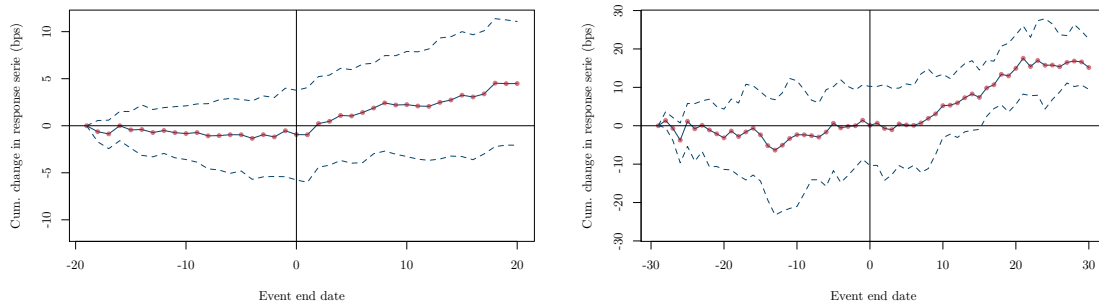


Figure 20: Average impact on 10 year sovereign yields

(a) Top 55 most damaging events (relative)

(b) Top 5 events (absolute)



Top 100 most costly events matching 55 series. The event time is date end of the event reported by EMDAT the window is 30 days. The series are controlled using constant mean correction.

Chief Editors

Pascal BLANQUÉ

Chief Investment Officer

Philippe ITHURBIDE

Senior Economic Advisor

DISCLAIMER

In the European Union, this document is only for the attention of “Professional” investors as defined in Directive 2004/39/EC dated 21 April 2004 on markets in financial instruments (“MIFID”), to investment services providers and any other professional of the financial industry, and as the case may be in each local regulations and, as far as the offering in Switzerland is concerned, a “Qualified Investor” within the meaning of the provisions of the Swiss Collective Investment Schemes Act of 23 June 2006 (CISA), the Swiss Collective Investment Schemes Ordinance of 22 November 2006 (CISO) and the FINMA’s Circular 08/8 on Public Advertising under the Collective Investment Schemes legislation of 20 November 2008. In no event may this material be distributed in the European Union to non “Professional” investors as defined in the MIFID or in each local regulation, or in Switzerland to investors who do not comply with the definition of “qualified investors” as defined in the applicable legislation and regulation. This document is not intended for citizens or residents of the United States of America or to any «U.S. Person» , as this term is defined in SEC Regulation S under the U.S. Securities Act of 1933.

This document neither constitutes an offer to buy nor a solicitation to sell a product, and shall not be considered as an unlawful solicitation or an investment advice.

Amundi accepts no liability whatsoever, whether direct or indirect, that may arise from the use of information contained in this material. Amundi can in no way be held responsible for any decision or investment made on the basis of information contained in this material. The information contained in this document is disclosed to you on a confidential basis and shall not be copied, reproduced, modified, translated or distributed without the prior written approval of Amundi, to any third person or entity in any country or jurisdiction which would subject Amundi or any of “the Funds”, to any registration requirements within these jurisdictions or where it might be considered as unlawful. Accordingly, this material is for distribution solely in jurisdictions where permitted and to persons who may receive it without breaching applicable legal or regulatory requirements.

The information contained in this document is deemed accurate as at the date of publication set out on the first page of this document. Data, opinions and estimates may be changed without notice. These data have been analyzed anonymously for scientific, statistical or historical research purposes.

You have the right to receive information about the personal information we hold on you. You can obtain a copy of the information we hold on you by sending an email to info@amundi.com. If you are concerned that any of the information we hold on you is incorrect, please contact us at info@amundi.com

Document issued by Amundi Asset Management, “société par actions simplifiée”- SAS with a capital of €1,086,262,605 - Portfolio manager regulated by the AMF under number GP04000036 - Head office: 90 boulevard Pasteur - 75015 Paris - France - 437 574 452 RCS Paris - www.amundi.com

Photo credit: iStock by Getty Images - monsitj/Sam Edwards